



HAL
open science

Triangulating submanifolds: An elementary and quantified version of Whitney's method

Jean-Daniel Boissonnat, Siargey Kachanovich, Mathijs Wintraecken

► To cite this version:

Jean-Daniel Boissonnat, Siargey Kachanovich, Mathijs Wintraecken. Triangulating submanifolds: An elementary and quantified version of Whitney's method. *Discrete and Computational Geometry*, 2020, 10.1007/s00454-020-00250-8 . hal-03109814

HAL Id: hal-03109814

<https://inria.hal.science/hal-03109814>

Submitted on 14 Jan 2021

HAL is a multi-disciplinary open access archive for the deposit and dissemination of scientific research documents, whether they are published or not. The documents may come from teaching and research institutions in France or abroad, or from public or private research centers.

L'archive ouverte pluridisciplinaire **HAL**, est destinée au dépôt et à la diffusion de documents scientifiques de niveau recherche, publiés ou non, émanant des établissements d'enseignement et de recherche français ou étrangers, des laboratoires publics ou privés.

Triangulating submanifolds: An elementary and quantified version of Whitney's method

J.-D. Boissonnat · S. Kachanovich · M. Wintraecken

Received: date / Accepted: date

Abstract We quantize Whitney's construction to prove the existence of a triangulation for any C^2 manifold, so that we get an algorithm with explicit bounds. We also give a new elementary proof, which is completely geometric.

Keywords Triangulations · Manifolds · Coxeter triangulations

1 Introduction

The question whether every C^1 manifold admits a triangulation was of great importance to topologists in the first half of the 20th century. This question was answered in the affirmative by Cairns [20], see also Whitehead [51]. However the first proofs were complicated and not very geometric, let alone algorithmic. It was Whitney [52, Chapter IV], who eventually gave an insightful geometric constructive proof. Here, we will be reproving Theorem 12A of [52, Section IV.12], in a more quantitative/algorithmic fashion for C^2 manifolds:

Theorem 1 *Every compact n -dimensional C^2 manifold \mathcal{M} embedded in \mathbb{R}^d admits a triangulation.*

This work has been funded by the European Research Council under the European Unions ERC Grant Agreement number 339025 GUDHI (Algorithmic Foundations of Geometric Understanding in Higher Dimensions). The third author also received funding from the European Union's Horizon 2020 research and innovation programme under the Marie Skłodowska-Curie grant agreement No. 754411.

J.-D. Boissonnat
Université Côte d'Azur, INRIA Sophia-Antipolis
Tel.: +33(0)4 92 38 77 60
E-mail: jean-daniel.boissonnat@inria.fr

Sargey Kachanovich
Université Côte d'Azur, INRIA Sophia-Antipolis
E-mail: siargey.kachanovich@inria.fr

Mathijs Wintraecken
IST Austria
E-mail: m.h.m.j.wintraecken@gmail.com

We note that C^2 -manifolds have positive reach, see [36]. The reach $\text{rch}(\mathcal{M})$ was introduced by Federer [36], as the minimal distance between a set \mathcal{M} (in this paper always a manifold) and its medial axis.

By more quantitative, we mean that instead of being satisfied with the existence of constants that are used in the construction, we want to provide explicit bounds in terms of the reach of the manifold, which we shall assume to be positive. The medial axis consists of points in ambient space that do not have a unique closest point on \mathcal{M} . Federer [36, Remark 4.20] also mentions that manifolds are of positive reach if and only if they are $C^{1,1}$. It is not too difficult to generalize the precise quantities to the setting where the manifold is $C^{1,1}$ (instead of C^2) at a small cost, see Appendix C.

Note that Theorem 1 implies that any C^1 manifold admits a triangulation. This is because any C^1 manifold can be smoothed (see for example [37]) and Whitney's own embedding theorem (see [52, Section IV.1]) gives a smooth embedding in \mathbb{R}^d .

Triangulations in computational geometry and topology are most often based on Voronoi diagrams and their dual Delaunay triangulations of the input point set, see for example [21, 10, 24, 9, 27] for general references in low dimensions and more recent work on manifolds embedded in higher dimensional spaces [16, 23].

Whitney's construction is of a quite different nature. He uses an ambient triangulation and constructs the triangulation of the manifold \mathcal{M} based on the intersections of \mathcal{M} with this triangulation. In this paper, we have chosen this ambient triangulation $\tilde{\mathcal{T}}$ to be (a perturbation of) a Coxeter triangulation \mathcal{T} of type \tilde{A}_d . A Coxeter triangulation of type \tilde{A}_d is Delaunay protected, a concept we'll recall in detail in Section 4. Delaunay protection gives that the triangulation is stable under perturbations. This property simplifies the proof, which in fact was one of the motivations for our choice. Moreover, Coxeter triangulations can be stored very compactly, in contrast with previous work [16, 23] on Delaunay triangulations.

The approach of the proof of correctness of the method, that we present in this paper, focuses on proving that after perturbing the ambient triangulation the intersection of each d -simplex in the triangulation $\tilde{\mathcal{T}}$ with \mathcal{M} is a slightly deformed n -dimensional convex polytope, more precisely the intersection is piecewise smoothly homeomorphic to a polytope. Proving this is the core of the homeomorphism proof in Section 7. The triangulation K of \mathcal{M} consists of a barycentric subdivision of a straightened version of these polytopes. This may remind the reader of the general result on CW-complexes, see [40], which was exploited by Edelsbrunner and Shah [35] for their triangulation result.

In this paper we construct 'normals' and a tubular neighbourhood for K that is compatible with the ambient triangulation $\tilde{\mathcal{T}}$ and prove that the projection along these 'normals' is a homeomorphism. This interpretation of Whitney's triangulation method is different from Whitney's original proof where the homeomorphism is given by the closest point projection and uses techniques which we also exploited in [15]. The homeomorphism we give in this paper is in fact piecewise smooth. We stress that this result is stronger than if we had based our work on the closed ball property of Edelsbrunner and Shah, which given criteria for a homeomorphism, but not for a piecewise linear/smooth homeomorphism nor an explicit map. We also believe that the tubular neighbourhood we construct is of independent interest. Because we have a bound on the size of the tubular neighbourhood of K and \mathcal{M} lies in this neigh-

bourhood, we automatically bound the Hausdorff distance between the two. A bound on the difference between the normals of K and \mathcal{M} is also provided. Thanks to our choice of ambient triangulation and our homeomorphism proof, this entire paper is elementary in the sense that no topological results are needed, all arguments are geometrical.

In addition to the more quantitative/algorithmic approach, the purely geometrical homeomorphism proof, the link with the closed ball property, the tubular neighbourhood for the triangulation K , and a bound on the Hausdorff distance, we also give different proofs for a fair number of Whitney's intermediate results.

In spite of this paper not being a review, the authors hope that it will serve to spread awareness of the classical work by Whitney [52] in the computational geometry and applied math communities. The main reason for this is that a large number of authors has reintroduced (weaker) versions of Whitney's concepts and results, without having been aware of the original.

The marching cube algorithm and some of its variants [39, 44, 32, 5] provide ways to approximate a manifold that is the zero set of a function. We will call such a manifold an isomanifold. These algorithms use a subdivision of the ambient space into simplices or cubes and constructing a piecewise linear approximation of the isomanifold inside each simplex or cube. This coincides with Whitney's approach where he subdivides the ambient space into cubes, which he then subdivides into simplices and then approximates the manifold inside each simplex. The main difference is that Whitney needs a perturbation of the ambient triangulation to guarantee topological correctness, while (with the exception of [44, 14] in two and three dimensions) no topological correctness (homeomorphism) is proven for the marching cube algorithms. Whitney is also more general because he treats general manifolds and not just isomanifolds. Moreover Allgower and Georg [4, Theorem 15.4.1] assume that the isomanifold avoids simplices in the ambient triangulation whose dimension is strictly less than the codimension of the isomanifold to prove that the piecewise linear approximation of the manifold is itself a manifold. This idea also originates with Whitney, and will be discussed in detail below.

Whitney's idea of using a subdivision of ambient space as a scaffold to build a triangulation has also been adopted outside of the marching cube community, see for example [22]. In [22] the scaffolding is based on the Voronoi diagram of a point sample. This is unlike the ambient triangulation used by Whitney. The focus on three dimensional ambient space and a specific type of surface, instead of general manifolds of arbitrary dimension and codimension, further distinguishes it from Whitney's work. As mentioned above the idea to use barycentric subdivision to construct a triangulation has also been often used, such as in [40, 35].

The part of the algorithm described in this paper that constructs the triangulation (see part 2 of the algorithm in Section 2.1) and the data structure to store the ambient triangulation have been implemented, see [17] and [38]. The implementation of the perturbation scheme (see part 1 of the algorithm in Section 2.1) is not yet complete at the moment of writing.

2 The algorithm and overview

2.1 The algorithm (based on Whitney's construction)

The algorithm takes as input an n -dimensional C^2 manifold $\mathcal{M} \subset \mathbb{R}^d$ with reach $\text{rch}(\mathcal{M})$, and outputs the triangulation K of \mathcal{M} . The algorithm based on Whitney's construction consists of two parts: We will refer to the first part as the perturbation algorithm. The perturbation algorithm perturbs the vertices of the ambient triangulation which ensures that the intersection of the ambient simplices with the manifold is nice (the intersection is piecewise smoothly homeomorphic to a polytope as we'll prove in Section 7). The second part is where the triangulation is constructed and is based on barycentric subdivision of polytopes.

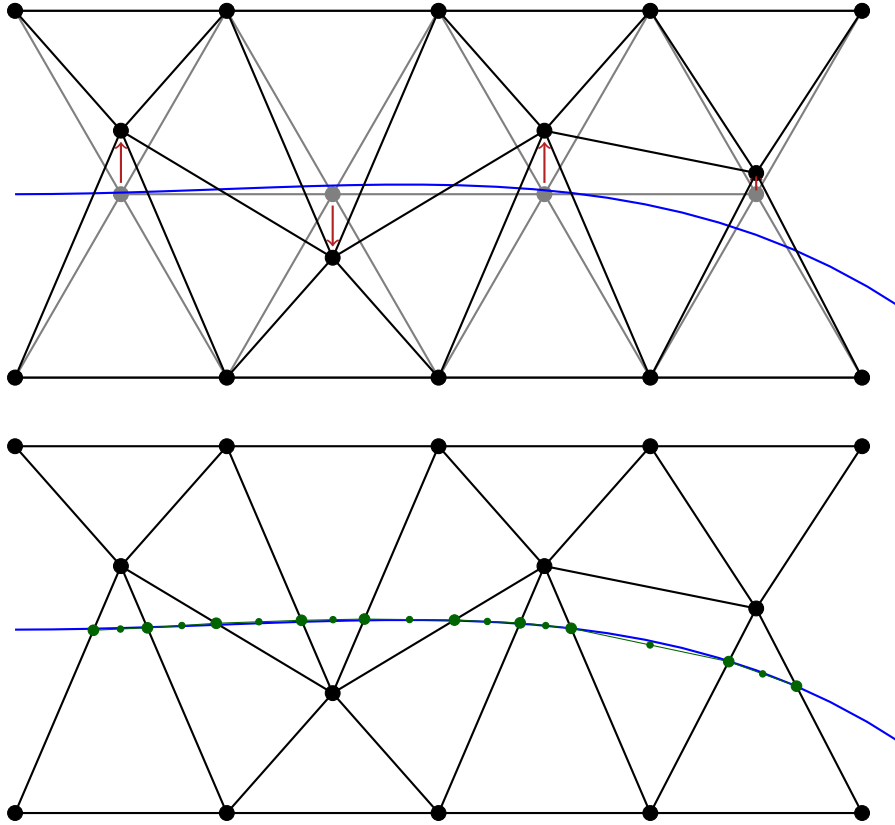


Fig. 1 The two parts of the algorithm: Part 1, where we perturb the vertices of the ambient triangulation, is depicted on top. Part 2, where the triangulation is constructed from the points of intersection of \mathcal{M} and the edges, is depicted below.

Part 1. (the perturbation algorithm) This part of the algorithm outputs a perturbed version of a Coxeter triangulation of \mathbb{R}^d of type \tilde{A}_d (see Section 4 for the

precise definition) and consists of two steps. In these two steps we have to carefully choose a significant number of parameters, which we will not discuss in detail in the global description of the algorithm. An overview of the most important parameters and notation can be found in Appendix A.

- Choose a Coxeter triangulation \mathcal{T} of type \tilde{A}_d of \mathbb{R}^d that is sufficiently fine. Here by fine we mean as determined by the longest edge length L . The longest edge length L is linear in the reach and depends in a rather intricate manner on the thickness (minimal altitude over longest edge length) of the top dimensional simplices in \tilde{A}_d and the dimension and codimension of the manifold. The precise expression will be given in (13).
- Perturb the vertices of \mathcal{T} slightly into a $\tilde{\mathcal{T}}$ (with the same combinatorial structure), such that all simplices in $\tilde{\mathcal{T}}$ of dimension at most $d - n - 1$ are sufficiently far away from the manifold. Here slightly is in terms of quality, protection (see Section 4 for the definitions) of the ambient triangulation as well as the longest edge length, separation, and dimension, see (19) for the precise bounds. Sufficiently far means some small fraction of the longest edge length and thus even smaller fraction of the reach of \mathcal{M} . The precise bound can be found in (16). This is done as follows: One maintains a list $\tilde{\mathcal{T}}_i$ of vertices and simplices, starting with an empty list and adding perturbed vertices while keeping the combinatorial structure of \mathcal{T} intact. This means that if $\tau = \{v_{j_1}, \dots, v_{j_k}\}$ is a simplex in \mathcal{T} and $\tilde{v}_{j_1}, \dots, \tilde{v}_{j_k} \in \tilde{\mathcal{T}}_i$, where \tilde{v}_i denotes the perturbed vertex v_i , then $\tilde{\tau} = \{\tilde{v}_{j_1}, \dots, \tilde{v}_{j_k}\}$ is a simplex in $\tilde{\mathcal{T}}_i$. We shall think of $\tilde{\mathcal{T}}_i$ simultaneously as list, simplicial complex, and a triangulation of a subset of \mathbb{R}^d . We shall think of i as the index of the vertex that was added last. To this list $\tilde{\mathcal{T}}_i$, one first adds all vertices v_i of \mathcal{T} such that $d(v_i, \mathcal{M}) \geq \frac{3}{2}L$, as well as the simplices with these vertices (see Case 1 of Section 5.2). For a vertex v_i such that $d(v_i, \mathcal{M}) < \frac{3}{2}L$ (Case 2), one goes through the following procedure. We first pick a point $p \in \mathcal{M}$ that is not too far from v_i . We then consider all $\tau'_j \subset \tilde{\mathcal{T}}_{i-1}$ of dimension at most $d - n - 2$, such that the join¹ $v_i * \tau'_j$ lies in $\tilde{\mathcal{T}}_i$. For all such τ'_j we consider $\text{span}(\tau'_j, T_p \mathcal{M})$ and we pick our perturbed v_i , that is \tilde{v}_i , such that it lies sufficiently far from the union of these spans, but also not too far from v_i (as we mentioned at the beginning). Here sufficiently far means a very small fraction of the longest edge length, see (22). The existence of such a point can be proven by volume estimates and is shown in Lemma 21. The fact that such a perturbation ensures that the $d - n - 1$ -skeleton is sufficiently far away from the manifold is non-trivial and proven in Lemma 22.

We note that for a curve in 2 dimensions, as depicted in Figure 1, or more generally a manifold of codimension 1, the set of all $\tau'_j \subset \tilde{\mathcal{T}}_{i-1}$ of dimension at most $d - n - 2$ is the empty set and $\text{span}(\tau'_j, T_p \mathcal{M})$ is $T_p \mathcal{M}$. The perturbation therefore ensures that \tilde{v}_i lies far from $T_p \mathcal{M}$.

Note that we only require limited knowledge of the manifold. Given a vertex v_i we need to be able to find a point on \mathcal{M} that is close to v_i or know if v_i is far from \mathcal{M} and we need access to $T \mathcal{M}$ in a finite sufficiently dense set of points (so that for

¹ The join of a simplex and a vertex is the convex hull of the vertices of the original simplex as well as the new vertex. Generally the join of two subsets $A, B \subset \mathbb{R}^d$, is defined as $A * B = \{\lambda a + \mu b \mid a \in A, b \in B\}$, where $\lambda, \mu \in \mathbb{R}$, $\lambda, \mu \geq 0$, and $\lambda + \mu = 1$, see for example [47, Chapter 1].

every point v_i that is close to \mathcal{M} we have a linear approximation of \mathcal{M}). We assume we have two oracles for the two operations. There are no fundamental difficulties in including small uncertainties in our knowledge of the close points or the tangent spaces, but the analysis would be more complicated. If we can sample \mathcal{M} densely finding close points is algorithmically not difficult. Methods to estimate the tangent space have been described in [2]. The same paper also describes estimates on the curvature. The estimate of the reach is discussed in [30] in three dimensions and [1] in high dimensions.

Complexity of part 1. The complexity of the perturbation (per vertex) of the algorithm is dominated by the number of simplices τ'_j that we have to consider. This number is bounded by the number of simplices of dimension at most $d - n - 2$ in the star of a vertex in a Coxeter triangulation plus 1, see (6) below. The number of simplices in turn is bounded by $(d - n)^d d^{(d-n)}$, see Lemma 17. This compares favourably with the complexity of the perturbation method in [11] for Delaunay triangulations, which is of order $\mathcal{O}(2^{d^2})$. A full analysis of the complexity of the algorithm, including basic operations on Coxeter triangulations, will be reported upon in a separate paper.

Part 2. (the triangulation construction) The construction of the triangulation of \mathcal{M} is now straightforward barycentric subdivision, for each $\tau^k \in \tilde{\mathcal{T}}$, of dimension k that contains a part of \mathcal{M} , we pick a point $v(\tau^k)$ in τ^k , see (28). For any sequence $\tau^{d-n} \subset \tau^{d-n+1} \subset \dots \subset \tau^d$, such that all simplices in the sequence intersect \mathcal{M} we add a simplex $\{v(\tau^{d-n}), \dots, v(\tau^d)\}$ to a simplicial complex K . If we have done this for all simplices that contain \mathcal{M} , K is a triangulation of \mathcal{M} .

For this second part we need an oracle that is able to tell us if the intersection between \mathcal{M} and $\tau^{d-n} \in \tilde{\mathcal{T}}$ is non-empty and if so, gives us the point of intersection. As we'll see in Section 6.1, it would in fact suffice to be able to find intersections between tangent planes and simplices.

2.2 A nice byproduct

The triangulation algorithm does not only provide a triangulation of the manifold itself, with simplices whose quality is lower bounded. It in fact immediately gives that the barycentric subdivision of the ambient triangulation contains a triangulation of the manifold. To ensure that the triangulation of the manifold is geometrically close to the manifold, we need to shift (some of the) vertices to the position that is computed by the algorithms above, see Figure 2. Because of the simplices of the triangulation of the manifold have good quality, we find a triangulation of the ambient space whose simplices have good quality. This byproduct may be of interest for finding solutions to numerical partial differential equations, in particular space time methods [48, 6, 49]. This also serves as a first step in generalizing the work on the triangulation of general stratifolds in three dimensions [43, 46, 31, 29, 28], which may be of interest given the effort that went into the detection of strata in arbitrary dimension, see for example [8, 7, 19].

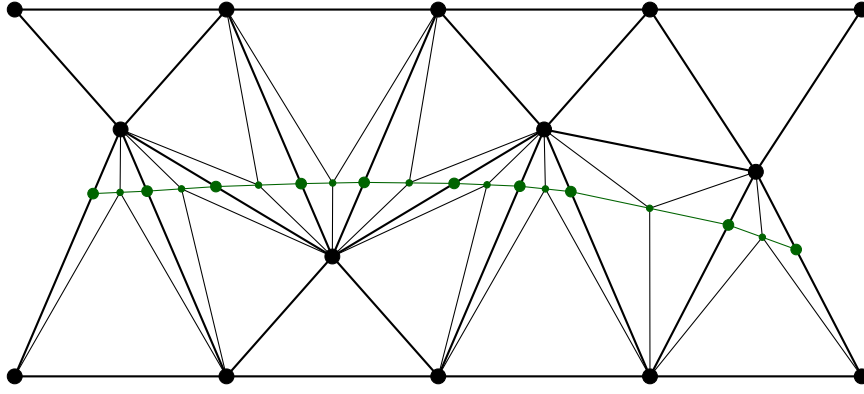


Fig. 2 The same triangulation as depicted in Figure 1 with the addition of simplices of the barycentric subdivision of the ambient triangulation added for the simplices that intersect the manifold.

2.3 Outline and overview of the proof

This paper is dedicated to the correctness proof of the algorithm presented in Section 2.1. After some background sections dedicated to manifolds of positive reach and Coxeter triangulations and their stability under perturbations, we continue with the perturbation algorithm.

In Section 3 we recall some results on the geometry of manifolds of positive reach. Coxeter triangulations, Delaunay protection, and the combinatorial stability of a triangulation under perturbations is the topic of Section 4.

In Section 5, we both give the details of the perturbation of the vertices and some geometric consequences for the triangulation. In Section 6, the triangulation K of \mathcal{M} is defined and an important quality bound for the simplices is given. Section 7 is dedicated to proving that K is a triangulation of \mathcal{M} . The proof is quite different from the approach Whitney described, which uses the closest point projection onto \mathcal{M} . Here we construct a tubular neighbourhood and 'normals' around the triangulation K , which is adapted to the ambient triangulation $\tilde{\mathcal{T}}$. We then prove that the projection using these 'normals' gives a piecewise smooth homeomorphism from $\tau^d \cap \mathcal{M}$ to $\tau^d \cap K$, where $\tau^d \in \tilde{\mathcal{T}}$ is d -dimensional. Because the construction is compatible on the faces of d -dimensional simplices the global result immediately follows. A more detailed overview of the homeomorphism proof is given in Section 7.

3 Manifolds, tangent spaces, distances and angles

In this section, we discuss some general results that will be of use. The manifold $\mathcal{M} \subset \mathbb{R}^d$ is a compact C^2 manifold with reach $\text{rch}(\mathcal{M})$.

We adhere as much as possible to the same notation as used in [18]. The tangent bundle will be denoted by $T\mathcal{M}$, while the tangent space at a point p is written as $T_p\mathcal{M}$. Similarly, $N\mathcal{M}$ is the normal bundle and $N_p\mathcal{M}$ a normal space. Distances on the manifold will be indicated by $d_{\mathcal{M}}(\cdot, \cdot)$, while we write $d(\cdot, \cdot)$ for distances in the

ambient Euclidean space, and $|\cdot|$ for the length of vectors. A ball centred at x with radius r is denoted by $B(x, r)$.

For a point x in the ambient space such that $d(x, \mathcal{M}) < \text{rch}(\mathcal{M})$ the closest point projection onto \mathcal{M} is denoted by $\pi_{\mathcal{M}}(x)$. The orthogonal projection onto the tangent $T_p\mathcal{M}$ is denoted by $\pi_{T_p\mathcal{M}}(x)$.

We will use a result from [18], which improves upon previous works such as Niyogi, Smale and Weinberger [42]:

Lemma 2 (Lemma 6 and Corollary 3 of [18]) *Suppose that \mathcal{M} is C^2 and let $p, q \in \mathcal{M}$, then*

$$\angle(T_p\mathcal{M}, T_q\mathcal{M}) \leq \frac{d_{\mathcal{M}}(p, q)}{\text{rch}(\mathcal{M})} \quad \text{and} \quad \sin\left(\frac{\angle(T_p\mathcal{M}, T_q\mathcal{M})}{2}\right) \leq \frac{|p - q|}{2\text{rch}(\mathcal{M})}.$$

In Lemma 3 we prove that the projection onto the tangent space is a diffeomorphism in a neighbourhood of size the reach of the manifold. This improves upon previous results by Niyogi, Smale, and Weinberger [42] in terms of the size of the neighbourhood, and is a more quantitative version of results by Whitney [52].

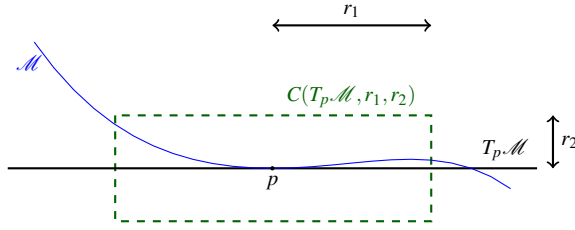


Fig. 3 The cylinder $C(T_p\mathcal{M}, r_1, r_2)$, with the manifold and tangent space.

We first recall some notation. Similarly to [18], we let $C(T_p\mathcal{M}, r_1, r_2)$ denote the ‘filled cylinder’ given by all points that project orthogonally onto a ball of radius r_1 in $T_p\mathcal{M}$ and whose distance to this ball is at most r_2 . We write $\mathring{C}(T_p\mathcal{M}, r_1, r_2)$ for the open cylinder. We refer to Figure 3 for an illustration. We now have:

Lemma 3 *Suppose that \mathcal{M} is C^2 and $p \in \mathcal{M}$, then for all $r < \text{rch}(\mathcal{M})$, the projection $\pi_{T_p\mathcal{M}}$ onto the tangent space $T_p\mathcal{M}$, restricted to $\mathcal{M} \cap \mathring{C}(T_p\mathcal{M}, r, \text{rch}(\mathcal{M}))$ is a diffeomorphism onto the open ball $B_{T_p\mathcal{M}}(r)$ of radius r in $T_p\mathcal{M}$, centred at p .*

Proof Apart from Lemma 2, we’ll be using the following results from [18]: For a minimizing geodesic γ on \mathcal{M} with length ℓ parametrized by arc length, with $\gamma(0) = p$ and $\gamma(\ell) = q$, we have

$$\angle\dot{\gamma}(0)\dot{\gamma}(t) \leq \frac{t}{\text{rch}(\mathcal{M})}. \quad (1)$$

If we also write $v_p = \dot{\gamma}(0)$, we see that

$$\begin{aligned}
\langle \gamma(\ell), v_p \rangle &= \int_0^\ell \frac{d}{dt} (\langle \gamma(t), v_p \rangle) dt \\
&= \int_0^\ell \langle \dot{\gamma}(t), t_0 \rangle dt \\
&\geq \int_0^\ell \cos\left(\frac{t}{\text{rch}(\mathcal{M})}\right) dt && \text{(using (1))} \\
&= \text{rch}(\mathcal{M}) \sin\left(\frac{\ell}{\text{rch}(\mathcal{M})}\right) \\
&\geq \text{rch}(\mathcal{M}) \sin(\angle(T_p\mathcal{M}, T_q\mathcal{M})), && \text{(using Lemma 2)}
\end{aligned}$$

as long as $\ell < \frac{1}{2}\text{rch}(\mathcal{M})\pi$. Because $v_p \in T_p\mathcal{M}$ and $\gamma(\ell) = q$, we have

$$|p - \pi_{T_p\mathcal{M}}(q)| \geq \text{rch}(\mathcal{M}) \sin(\angle(T_p\mathcal{M}, T_q\mathcal{M})). \quad (2)$$

This means in particular that for all q such that $|p - \pi_{T_p\mathcal{M}}(q)| < \text{rch}(\mathcal{M})$ and $|q - \pi_{T_p\mathcal{M}}(q)| \leq \text{rch}(\mathcal{M})$ the angle between $T_p\mathcal{M}$ and $T_q\mathcal{M}$ is less than 90 degrees. This in turn implies that the Jacobian of projection map is non-degenerate. Note that the condition on ℓ mentioned above is satisfied by a combination of Theorem 1 and Lemma 11 of [18]. \square

It is clear by considering the sphere that this result is tight, in the sense that r cannot be chosen equal to $\text{rch}(\mathcal{M})$ for general manifolds. See Appendix C for some remarks on these results in the $C^{1,1}$ setting.

Definition 4 We shall write π_p as an abbreviation for the restriction (of the domain) of $\pi_{T_p\mathcal{M}}$ to $\mathcal{M} \cap \mathring{C}(T_p\mathcal{M}, \text{rch}(\mathcal{M}), \text{rch}(\mathcal{M}))$ and π_p^{-1} for its inverse.

We now also immediately have a quantitative version of Lemma IV.8a of [52]:

Corollary 5 Suppose that \mathcal{M} is C^2 and p in \mathcal{M} , then for all $r < \text{rch}(\mathcal{M})$

$$d(p, \mathcal{M} \setminus C(T_p\mathcal{M}, r, \text{rch}(\mathcal{M}))) = d(p, \mathcal{M} \setminus \pi_p^{-1}(B_{T_p\mathcal{M}}(r))) \geq r. \quad (3)$$

Proof Lemma 3 implies that $\pi_p^{-1}(B_{T_p\mathcal{M}}(r)) = \mathcal{M} \cap C(T_p\mathcal{M}, r, \text{rch}(\mathcal{M}))$. By definition of the filled cylinder we have that $d(p, \mathbb{R}^d \setminus C(T_p\mathcal{M}, r, \text{rch}(\mathcal{M}))) = r$. The result now follows. \square

We shall also need the following bound on the (local) distance between a tangent space and the manifold.

Lemma 6 (Distance to Manifold, Lemma 11 of [18]) Let \mathcal{M} be a manifold of positive reach. Suppose that $w \in T_p\mathcal{M}$ and $|w - p| < \text{rch}(\mathcal{M})$. Let $\pi_p^{-1}(w)$ be as in Definition 4. Then

$$|\pi_p^{-1}(w) - w| \leq \left(1 - \sqrt{1 - \left(\frac{|w - p|}{\text{rch}(\mathcal{M})}\right)^2}\right) \text{rch}(\mathcal{M}).$$

This is attained for the sphere of radius $\text{rch}(\mathcal{M})$.

4 Coxeter triangulations, Delaunay protection and stability

Coxeter triangulations [26] of Euclidean space play a significant role in our work. They combine many of the advantages of cubes, with the advantages of triangulations. They are also attractive from the geometrical perspective, because they provide simplices with very good quality and some particular Coxeter triangulations are Delaunay protected and thus very stable Delaunay triangulations. We will now very briefly introduce both the concepts of Coxeter triangulations and Delaunay protection, but refer to [25] for more details on Coxeter triangulations and to [11, 12] for Delaunay protection.

Definition 7 A *monohedral*² triangulation is called a Coxeter triangulation if all its d -simplices can be obtained by consecutive orthogonal reflections through facets of the d -simplices in the triangulation and the affine hulls of facets entirely consist of facets of d -simplices in the triangulation.

This definition imposes very strong constraints on the geometry of the simplices, implying that there are only a small number of such triangulations in each dimension. Most of these triangulations are part of 4 families for which there is one member for (almost) every dimension d . We will focus on one such family, \tilde{A}_d , which is Delaunay protected.

The simplest and shortest definition of a Coxeter triangulation of type \tilde{A}_d is to give it as a triangulation of a d -dimensional linear subspace of \mathbb{R}^{d+1} , by rotation

Definition 8 Let $P = \{(x^i) \in \mathbb{R}^{d+1} \mid \sum_i x^i = 0\}$ and consider the d -simplex with vertices u_k in P .

$$u_0 = \left(0^{\{d+1\}}\right) \quad u_k = \left(\left(-\frac{d+1-k}{d+1} \right)^{\{k\}}, \left(\frac{k}{d+1} \right)^{\{d+1-k\}} \right), \quad k \in [d],$$

where $x^{\{k\}}$ denotes k consecutive coordinates x . The Coxeter triangulation of type \tilde{A}_d in P is found by consecutively reflecting the simplex in its faces.

Protection.

Definition 9 The protection of a d -simplex σ in a Delaunay triangulation on a point set P is the minimal distance of points in $P \setminus \sigma$ to the circumscribed ball of σ :

$$\delta(\sigma) = \inf_{p \in P \setminus \sigma} d(p, B(\sigma)), \text{ where } B(\sigma) \text{ is the circumscribed ball of } \sigma.$$

The protection δ of a Delaunay triangulation \mathcal{T} is the infimum over the d -simplices of the triangulation: $\delta = \inf_{\sigma \in \mathcal{T}} \delta(\sigma)$. A Delaunay triangulation with a positive protection is called protected.

The proof that \tilde{A}_d triangulations are protected can be found in [25, Section 6]. We shall denote the triangulation of this type by \mathcal{T} .

Stability. In the triangulation proof below we need that a perturbation $\tilde{\mathcal{T}}$ of our initial ambient triangulation (\mathcal{T} of type \tilde{A}_d) is still a triangulation of \mathbb{R}^d . We shall

² A triangulation of \mathbb{R}^d is called *monohedral* if all its d -simplices are congruent.

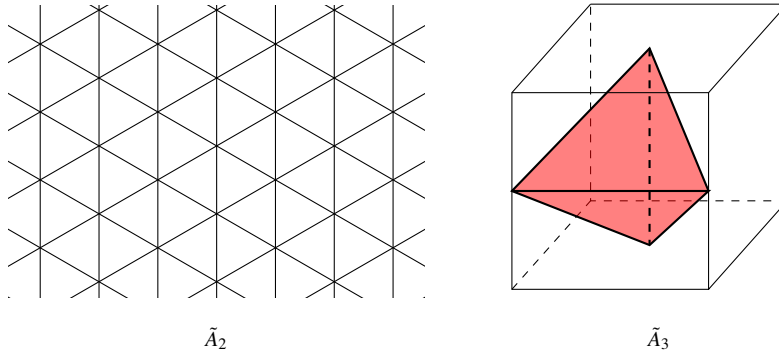


Fig. 4 The vertex sets of the Coxeter triangulations in dimensions two and three are the triangular lattice and the body-centred cubic lattice, respectively.

refer to this as (combinatorial) stability. Because Whitney did not use a protected Delaunay triangulation he needs a non-trivial topological argument to establish this, see [52, Appendix Section II.16]. The argument for stability of triangulations for \tilde{A} type Coxeter triangulations is much simpler, because it is a Delaunay triangulation and δ -protected, see [25]. Before we can recall this result we need to introduce some notation and a definition:

- The minimal altitude or height, denoted by minalt , is the minimum over all vertices of the altitude, that is the distance from a vertex to the affine hull of the opposite face. $t(\tau)$ denotes the thickness of a simplex τ , that is the ratio of the minimal altitude to the maximal edge length. We write $t(\mathcal{T})$ for infimum of the thickness over all simplices in \mathcal{T} .
- We can think of the vertices of \mathcal{T} as an (ε, μ) -net. Here μ is the separation (for Coxeter triangulations, the shortest edge length in \mathcal{T}), and ε the sampling density (which is the circumradius of the simplices in the Coxeter triangulation). We write μ_0 for the normalized separation, that is $\mu_0 = \frac{\mu}{\varepsilon}$.
- For any complex K , $L(K)$ denotes the longest edge length in K . We use the abbreviations $L = L(\mathcal{T})$ and $\tilde{L} = L(\tilde{\mathcal{T}})$.
- A perturbation of the vertices $\{v_i\}$ to $\{\tilde{v}_i\}$ is called an ε -perturbation if $|v_i - \tilde{v}_i| \leq \varepsilon$, for all i .

Theorem 4.14 of [11] immediately gives:

Corollary 10 *The triangulation \mathcal{T} is (combinatorially) stable under a $\tilde{c}L$ -perturbation as long as*

$$\tilde{c}L \leq \frac{t(\mathcal{T})\mu_0}{18d} \delta. \quad (4)$$

We claim the following concerning the behaviour of \tilde{c}

Lemma 11

$$\tilde{c} \leq \frac{t(\mathcal{T})\mu_0}{18d} \frac{\delta}{L} \leq \sqrt{2} \frac{\sqrt{d^2 + 2d + 24} - \sqrt{d^2 + 2d}}{9d^{3/2}\sqrt{d+2}(d+1)} \sim \frac{\sqrt{32}}{3d^4},$$

where \sim denotes equality up to the leading order in the asymptotic development.

Proof Choudhary et al. [25, Appendix B] provide explicit values of all the quantities mentioned in Corollary 10 for a Coxeter triangulation of type \tilde{A} , with the exception of μ , which can be easily derived from a more general result. If we fix the scale (which in [25] we did by a convenient choice of coordinates for the vertices), we have

$$\begin{aligned} L(\sigma) &= \begin{cases} \frac{\sqrt{d+1}}{2} & \text{if } d \text{ is odd,} \\ \frac{1}{2} \sqrt{\frac{d(d+2)}{(d+1)}} & \text{if } d \text{ is even} \end{cases} & t(\sigma) &= \begin{cases} \sqrt{\frac{2}{d}} & \text{if } d \text{ is odd,} \\ \sqrt{\frac{2(d+1)}{d(d+2)}} & \text{if } d \text{ is even} \end{cases} \\ \varepsilon &= \sqrt{\frac{d(d+2)}{12(d+1)}} & \delta(\sigma) &= \frac{\sqrt{d^2+2d+24} - \sqrt{d^2+2d}}{\sqrt{12(d+1)}}. \end{aligned} \quad (5)$$

The value of μ easily follows from the general expression of edge lengths (see [25, Appendix B, \tilde{A}_d , item 5]) and is equal to $\mu = \sqrt{\frac{d}{d+1}}$. From (5), we get that $\mu_0 = \frac{\mu}{\varepsilon} = \sqrt{\frac{12}{d+2}}$. The bound in (4) is therefore

$$\begin{aligned} \tilde{c} &\leq \frac{t(\sigma)\mu_0}{18d} \frac{\delta}{L} = \begin{cases} \frac{\sqrt{2} \sqrt{d^2+2d+24} - \sqrt{d^2+2d}}{9d^{3/2} \sqrt{d+2}(d+1)} & \text{if } d \text{ is odd,} \\ \frac{\sqrt{2(d+1)} \sqrt{d^2+2d+24} - \sqrt{d^2+2d}}{9d^2(d+2)^{3/2}} & \text{if } d \text{ is even.} \end{cases} \\ &\leq \sqrt{2} \frac{\sqrt{d^2+2d+24} - \sqrt{d^2+2d}}{9d^{3/2} \sqrt{d+2}(d+1)} \sim \frac{\sqrt{32}}{3d^4}, \end{aligned}$$

where we used that $\sqrt{1+x} \simeq 1 + \frac{1}{2}x$ if x is close to zero. \square

Thickness and angles. The quality of simplices and the control over the alignment of the simplices with the manifold is an essential part of the triangulation proof, for which we need two basic results. Similar statements can be found in Section IV.14 and Section IV.15 of [52].

We remind ourselves of the following:

Lemma 12 (Thickness under distortion [34, Lemma 7]) *Suppose that $\sigma = \{v_0, \dots, v_k\}$ and $\tilde{\sigma} = \{\tilde{v}_0, \dots, \tilde{v}_k\}$ are two k -simplices in \mathbb{R}^d such that $||v_i - v_j| - |\tilde{v}_i - \tilde{v}_j|| \leq c_0 L(\sigma)$ for all $0 \leq i < j \leq k$. If $c_0 \leq \frac{t(\sigma)^2}{4}$, then $t(\tilde{\sigma}) \geq \frac{4}{5\sqrt{k}} (1 - \frac{4c_0}{t(\sigma)^2}) t(\sigma)$.*

We can now state a variation of Whitney's angle bound result, see [52, Section IV.15].

Lemma 13 (Whitney's angle bound) *Suppose σ is a j -simplex of \mathbb{R}^d , $j < d$, whose vertices all lie within a distance d_{\max} from a k -dimensional affine space $A_0 \subset \mathbb{R}^d$ with $k \geq j$. Then*

$$\sin \angle(\text{aff}(\sigma), A_0) \leq \frac{(j+1)d_{\max}}{\min \text{alt}(\sigma)}.$$

Proof We first notice that the barycentre c_b of a simplex σ^j is at least a distance $\min \text{alt}(\sigma^j)/(j+1)$ removed from the faces of the simplex. This means that the ball in $\text{aff}(\sigma^j)$ centred on c with radius $\min \text{alt}(\sigma^j)/(j+1)$, denoted by $B_{\text{aff}(\sigma^j)}(c, \min \text{alt}(\sigma^j)/(j+1))$

1)), is contained in σ^j . We now consider any diameter, that is a line segment ℓ connecting a pair of antipodal points of $\partial B_{\text{aff}(\sigma^j)}(c, \min \text{alt}(\sigma^j)/(j+1))$. This diameter is contained in a d_{\max} neighbourhood of A_0 and thus

$$\sin \angle(\ell, A_0) \leq \frac{(j+1)d_{\max}}{\min \text{alt}(\sigma)}.$$

The result now follows, because ℓ is arbitrarily chosen. \square

Simplices in a star in a triangulation of type $\tilde{\mathbf{A}}_d$. The precise number of simplices in the star of a vertex plays an important role in the volume estimates in Section 5. We will now give an explicit bound on this number.

In general the $(d-k)$ -faces of a Voronoi cell correspond to the k -faces in the Delaunay dual. The triangulation \mathcal{T} is Delaunay and the dual of a vertex is a permutahedron, see [25]. We recall that the permutahedron is defined as follows:

Definition 14 (Permutahedron) *A d -permutahedron is a d -dimensional polytope, which is the convex hull \mathcal{P} of all points in \mathbb{R}^{d+1} , the coordinates of which are permutations of $\{1, \dots, d+1\}$.*

We also remind ourselves of the following definition, see [3], and corollary, see [41]:

Definition 15 *Let $S(d, k)$ be the Stirling number of the second kind, which is the number of ways to partition a set of d elements into k non-empty subsets, that is*

$$S(d, k) = \frac{1}{k!} \sum_{j=0}^k (-1)^j \binom{k}{j} (k-j)^d.$$

Corollary 16 (Corollary 3.15 of [41]) *The number of $(d+1-k)$ -faces of the permutahedron is $k!S(d+1, k)$.*

By duality, the lemma immediately gives us the number N_k of k -faces that contain a given vertex in \mathcal{T} , $N_k = k!S(d+1, k)$. We also write

$$N_{\leq k} = 2 + \sum_{j=1}^k j!S(d+1, j), \quad (6)$$

which is an upper bound on the total number of faces of dimension less or equal to k that contain a given vertex. We have added 2 because we want to have a safety margin if we have to consider the empty set (as will be apparent in (20)), and have a strict inequality. We now claim the following:

Lemma 17 *We have $N_{\leq k} \lesssim k^d d^k$.*

Proof Theorem 3 of [45] gives us that for $d \geq 2$ and $1 \leq j \leq d-1$

$$\frac{1}{2}(j^2 + j + 2)j^{d-j-1} - 1 \leq S(d, j) \leq \frac{1}{2} \binom{d}{j} j^{d-j}.$$

Furthermore, Stirlings theorem and the binomial theorem give that $j! \sim j^j$ and $\sum_{j=0}^k \binom{d}{j} \lesssim d^k$, respectively. We now see that

$$N_{\leq k} = 2 + \sum_{j=1}^k j! S(d+1, j) \lesssim \sum_{j=1}^k j! \binom{d+1}{j} j^{d+1-j} \lesssim k^d \sum_{j=1}^k \binom{d}{j} \lesssim k^d d^k.$$

It is clear that if k is much smaller than d that then k^d dominates. □

5 Perturbing the ambient triangulation

This section is dedicated to the perturbation of the Coxeter triangulation such that the manifold is sufficiently far from the simplices of dimension at most $d - n - 1$ in $\tilde{\mathcal{T}}$.

- In Section 5.1, we prove that it is possible to perturb the points as described in the second step of part 1 of the algorithm. This involves a significant amount of volume estimates, which are completely quantized. We also indicate how fine the ambient triangulation \mathcal{T} has to be compared to $\text{rch}(\mathcal{M})$; the longest edge length is linear in terms of the reach (the dependence on the dimension and codimension is rather complicated).
- In Section 5.2, we define the perturbation and prove that this in fact gives a triangulation for which the low dimensional simplices lie sufficiently far from the manifold.

The proofs of the results in Section 5.2 rely on Appendix B. We shall indicate the corresponding sections in Whitney [52], when appropriate.

5.1 The complex $\tilde{\mathcal{T}}$

Before we can dive into the algorithmic construction of the perturbed complex $\tilde{\mathcal{T}}$, we need to fix some constants and give some explicit bounds on the constants. This subsection corresponds to Section IV.18 of [52].

Balls and exclusion volumes. Let $B^d(r)$ be any ball in \mathbb{R}^d of radius r . We now define $\bar{\rho}_1 > 0$ as follows: For any two parallel $(d-1)$ -hyperplanes whose distance apart is less than $2\bar{\rho}_1 r$, the intersection of the slab between the two hyperplanes with the ball $B^d(r)$ is denoted by \mathcal{S} . Now, $\bar{\rho}_1$ is the largest number such that the volume (vol) of any \mathcal{S} satisfies

$$\text{vol}(\mathcal{S}) \leq \frac{\text{vol}(B^d(r))}{2N_{\leq d-n-1}},$$

with $N_{\leq d-n}$ as in (6).

A precise bound on $\bar{\rho}_1$ can be given, see Remark 1 below. We will use an easier bound ρ_1 , at the cost of weakening the result:

Lemma 18 *We have*

$$\bar{\rho}_1 \geq \rho_1 = \begin{cases} \frac{2^{2k-2}(k!)^2}{\pi(2k)!N_{\leq d-n-1}} & \text{if } d = 2k \\ \frac{(2k)!}{2^{2k+2}k!(k-1)!N_{\leq d-n-1}} & \text{if } d = 2k-1. \end{cases} \quad (7)$$

Note that

$$\rho_1 \sim \frac{1}{\sqrt{d}N_{\leq d-n-1}}.$$

Proof We can bound the volume of the slab \mathcal{S} by the cylinder with base $B_{d-1}(r)$ and height $2\rho_1 r$, that is

$$2\rho_1 r^d \frac{\pi^{\frac{d-1}{2}}}{\Gamma(\frac{d+1}{2})}.$$

This means that

$$\begin{aligned} \frac{\text{vol}(\mathcal{S})}{\text{vol}(B^d(r))} &< \frac{2\rho_1 r \text{vol}(B_{d-1}(r))}{\text{vol}(B^d(r))} \\ &= \frac{2\rho_1 \frac{\pi^{\frac{d-1}{2}}}{\Gamma(\frac{d-1}{2}+1)}}{\frac{\pi^{\frac{d}{2}}}{\Gamma(\frac{d}{2}+1)}} \\ &= \frac{2\rho_1 \Gamma(\frac{d}{2}+1)}{\sqrt{\pi} \Gamma(\frac{d-1}{2}+1)} \\ &= \begin{cases} \frac{\pi(2k)!}{2^{2k-1}(k!)^2} \rho_1 & \text{if } d = 2k \\ \frac{2^{2k+1}k!(k-1)!}{(2k)!} \rho_1 & \text{if } d = 2k-1. \end{cases} \end{aligned}$$

using the standard formulae for the volume of the ball, see for example [33, page 622]. Note that the inequality is strict because $\rho_1 > 0$. We see that therefore ρ_1 may be chosen to be

$$\rho_1 = \begin{cases} \frac{2^{2k-2}(k!)^2}{\pi(2k)!N_{\leq d-n-1}} & \text{if } d = 2k \\ \frac{(2k)!}{2^{2k+2}k!(k-1)!N_{\leq d-n-1}} & \text{if } d = 2k-1. \end{cases} \quad (7)$$

From Wendel's bound on the ratio of Gamma functions [50], we immediately see that for a fixed constant a ,

$$\frac{\Gamma(x+a)}{\Gamma(x)} \sim x^a.$$

This means that

$$\frac{2\rho_1 \Gamma(\frac{d}{2}+1)}{\sqrt{\pi} \Gamma(\frac{d-1}{2}+1)} \sim \frac{2\rho(\frac{d}{2}+\frac{1}{2})^{1/2}}{\sqrt{\pi}} \sim \sqrt{d}.$$

We now see that

$$\rho_1 \sim \frac{1}{\sqrt{d}N_{\leq d-n-1}}.$$

□

Remark 1 Because of symmetry, the largest volume \mathcal{S} can attain is when both delimiting hyperplanes are equidistant to the center of $B^d(r)$. The volume of \mathcal{S} is given by the integral

$$r^d \int_{-\bar{\rho}_1}^{\rho_1} \text{vol} \left(B_{d-1} \left(\sqrt{1-h^2} \right) \right) dh = \frac{\pi^{\frac{d-1}{2}}}{\Gamma(\frac{d+1}{2})} r^d \int_{-\rho_1}^{\rho_1} \left(\sqrt{1-h^2} \right)^{d-1} dh,$$

where $B_{d-1}(r)$ denotes the ball of dimension $d-1$ with radius r and Γ denotes the Euler gamma function. This integral can be expressed using special functions such as the hypergeometric function or beta functions. This gives an explicit value for $\bar{\rho}_1$.

The coarseness of \mathcal{T} . As mentioned, we perturb the vertices of a Coxeter triangulation. The maximal distance that we allow between an unperturbed vertex v_i and the associated perturbed vertex \tilde{v}_i is $\tilde{c}L$. We define \tilde{c} as

$$\tilde{c} = \min \left\{ \frac{t(\mathcal{T})\mu_0\delta}{18dL}, \frac{1}{24}t(\mathcal{T})^2 \right\}. \quad (8)$$

The reasons for this particular choice will be discussed after (19) below. We stress that (8) is independent of L because δ scales linearly with L . Notice that because $t(\mathcal{T}) \leq 1$, by definition of the thickness of a simplex, we have

$$\tilde{c} \leq \frac{1}{24}. \quad (9)$$

We are now ready to introduce the demands on the triangulation of ambient space. We start by bounding the scale of the Coxeter triangulation \mathcal{T} by bounding the longest edge length. We do this by giving some constants. We define α_1 and α_k by a recursion relation as follows

$$\alpha_1 = \frac{4}{3}\rho_1\tilde{c} \quad \frac{2}{3}\alpha_{k-1}\tilde{c}\rho_1 = \alpha_k, \quad (10)$$

that is $\alpha_k = \frac{2^{k+1}}{3^k}\rho_1^k\tilde{c}^k$. These definitions play an essential role in the volume estimates for the perturbation of the vertices, that are necessary to guarantee quality. Note that α_k is extremely small. In particular, we shall have that

$$\alpha_k \leq \frac{1}{18^k}, \quad (11)$$

because $\tilde{c} \leq \frac{1}{24}$, as we have seen in (9). ρ_1 is also very small, as a direct consequence of Lemma 18. Furthermore we notice that $\alpha_k < \alpha_{k-1}$. To make sure the formulae do not become too big, we introduce the notation

$$\zeta = \frac{8}{15\sqrt{d} \binom{d}{d-n} \cdot (1+2\tilde{c})} \left(1 - \frac{8\tilde{c}}{t(\mathcal{T})^2} \right) t(\mathcal{T}). \quad (12)$$

Note that ζ depends on both the ambient and intrinsic dimension and the perturbation parameter \tilde{c} . Because $\tilde{c} \leq \frac{1}{24}t(\mathcal{T})^2$ and $t(\mathcal{T}) \leq 1$ we see that $\zeta \leq 1$. We set the coarseness of the ambient triangulation by demanding that L satisfies

$$\left(1 - \sqrt{1 - \left(\frac{6L(\mathcal{T})}{\text{rch}(\mathcal{M})}\right)^2}\right) \text{rch}(\mathcal{M}) = \frac{(\alpha_{d-n})^{4+2n}}{6(n+1)^2} \zeta^{2n} L, \quad (13)$$

or equivalently

$$\frac{L}{\text{rch}(\mathcal{M})} = \frac{2 \frac{(\alpha_{d-n})^{4+2n}}{6(n+1)^2} \zeta^{2n}}{\left(\frac{(\alpha_{d-n})^{4+2n}}{6(n+1)^2} \zeta^{2n}\right)^2 + 6^2}. \quad (14)$$

Note that

$$\frac{L}{\text{rch}(\mathcal{M})} < \frac{(\alpha_{d-n})^{4+2n}}{54(n+1)^2} \zeta^n < \frac{(\alpha_{d-n})^2}{54}, \quad \frac{(\alpha_{d-n})^{4+2n}}{6(n+1)^2} \zeta^{2n} < \frac{(\alpha_{d-n})^2}{3} \leq \frac{\alpha_{d-n}}{3}, \quad (15)$$

where we used that $\zeta \leq 1$, which will often be used below to simplify expressions.

Remark 2 We have to choose the right hand side in (13) very small, because the bounds on the quality of the simplices that will make up the triangulations are very weak. The details of these estimates can be found in Lemma 28.

$(d-n-1)$ -skeleton safe triangulations. We shall denote the simplices by τ and σ . We will use lower indices to distinguish simplices, while upper indices will stress the dimension, for example τ_j^k is a simplex of dimension k .

Definition 19 ($(d-n-1)$ -skeleton safe triangulations) *We say that a perturbed triangulation $\tilde{\mathcal{T}}$ of \mathcal{T} in \mathbb{R}^d is $(d-n-1)$ -skeleton safe with respect to the n -dimensional manifold \mathcal{M} if*

$$d(\tau^k, \mathcal{M}) > \alpha_k L, \quad (16)$$

for all faces τ^k in $\tilde{\mathcal{T}}$, with $k \leq d-n-1$, and

$$\tilde{L} < \frac{13}{12} L \quad (17)$$

$$t(\tilde{\mathcal{T}}) \geq \frac{4}{5\sqrt{d}} \left(1 - \frac{8\tilde{c}}{t(\mathcal{T})^2}\right) t(\mathcal{T}). \quad (18)$$

5.2 Perturbing the vertices

We now discuss the details of the perturbation scheme that we described in the algorithm section. The perturbation scheme follows Whitney [52, Section IV.18] and is inductive.

Construction of $\tilde{\mathcal{T}}$. Let v_1, v_2, \dots be the vertices of \mathcal{T} , we are going to inductively choose new vertices $\tilde{v}_1, \tilde{v}_2, \dots$ for $\tilde{\mathcal{T}}$, with

$$|v_i - \tilde{v}_i| \leq \tilde{c}L = \min \left\{ \frac{t(\mathcal{T})\mu_0}{18d} \delta, \frac{1}{24} t(\mathcal{T})^2 L \right\}, \quad (19)$$

using the notation of Section 4. With this bound we have that (17) is satisfied, because the two vertices of an edge are perturbed by at most $\tilde{c}L$ and thus the triangle inequality yields $\tilde{L} \leq (1 + 2\tilde{c})L$. We also claim the following:

Lemma 20 *$\tilde{\mathcal{T}}$ has the same combinatorial structure as \mathcal{T} . Moreover, (18) is satisfied.*

Proof Because we assume that the perturbation is sufficiently small compared to the protection, as given in the first condition of (19), (4) is satisfied and $\tilde{\mathcal{T}}$ will have exactly the same combinatorial structure as \mathcal{T} .

By the third condition of (19) we have a lower bound on the quality of the simplices. To be precise, we have that for any simplex τ in $\tilde{\mathcal{T}}$

$$t(\tau) \geq \frac{4}{5\sqrt{d}} \left(1 - \frac{8\tilde{c}}{t(\mathcal{T})^2} \right) t(\mathcal{T}), \quad (18)$$

as a consequence of Lemma 12, the fact that if you perturb the vertices by $\tilde{c}L$ the edge lengths are perturbed $2\tilde{c}$ (that is $2\tilde{c} = c_0$) and the fact that if $\sigma \subset \tau$, then $t(\sigma) \geq t(\tau)$. So we have established (18). \square

We now give the scheme where the vertices are perturbed inductively. Suppose that the vertices $\tilde{v}_1, \dots, \tilde{v}_{i-1}$ have been determined, and thus the complex $\tilde{\mathcal{T}}_{i-1}$ with these vertices. A simplex $\{\tilde{v}_{j_1} \dots \tilde{v}_{j_k}\}$ lies in $\tilde{\mathcal{T}}_{i-1}$ if and only if $\{v_{j_1} \dots v_{j_k}\}$ lies in \mathcal{T} . We shall now find \tilde{v}_i and thus $\tilde{\mathcal{T}}_i$ so that for any $\tau^k \in \tilde{\mathcal{T}}_i$ of dimension $k \leq d - n - 1$, (16) is satisfied. We distinguish two cases:

Case 1 ($d(v_i, \mathcal{M}) \geq \frac{3}{2}L$). In this case we choose $\tilde{v}_i = v_i$. The inequality (16) is established as follows: Because $\tilde{L} < (1 + 2\tilde{c})L$, which means that for any point x in the star of $\tilde{v}_i = v_i$ we have $d(x, \tilde{v}_i (= v_i)) < (1 + 2\tilde{c})L$. By the triangle inequality we see that $d(x, \mathcal{M}) \geq d(v_i, \mathcal{M}) - d(x, \tilde{v}_i (= v_i)) \geq (\frac{1}{2} - 2\tilde{c})L$. That is, any simplex in $\tilde{\mathcal{T}}$ with vertex $\tilde{v}_i = v_i$ is at least distance $(\frac{1}{2} - 2\tilde{c})L$ from the manifold. Thanks to (9) we have that $(\frac{1}{2} - 2\tilde{c})L > \frac{5}{12}L$. This means that $d(\tau^k, \mathcal{M}) > \frac{5}{12}L$ for any simplex in the star of $\tilde{v}_i = v_i$. This lower bound is much larger than $\alpha_k L < \frac{1}{18^k}L$.

Case 2 ($d(v_i, \mathcal{M}) < \frac{3}{2}L$). Let p be a point in \mathcal{M} such that $d(v_i, p) < \frac{3}{2}L$. Let

$$\tau'_0 (= \emptyset), \tau'_1, \dots, \tau'_v \quad (20)$$

be the simplices of $\tilde{\mathcal{T}}_{i-1}$ such that the joins $\tau_j = \tau'_j * \tilde{v}_i$ are simplices of $\tilde{\mathcal{T}}$, and $\dim(\tau'_j * \tilde{v}_i) \leq d - n - 1$ (and thus $\dim(\tau'_j) \leq d - n - 2$), with $0 \leq j \leq v$. We note

that $v \leq N_{\leq d-n-1}$, with $N_{\leq k}$ as defined in (6). We now consider the span, denoted by $\text{span}(\tau'_j, T_p \mathcal{M})$, for all $0 \leq j \leq v$. Note that the dimension of $\text{span}(\tau'_j, T_p \mathcal{M})$ is at most $(d-n-2) + n + 1 = d-1$.

We now claim the following:

Lemma 21 *We can pick \tilde{v}_i such that it lies sufficiently far from each $\text{span}(\tau'_j, T_p \mathcal{M})$, that is*

$$d(\tilde{v}_i, \text{span}(\tau'_j, T_p \mathcal{M})) \geq \rho_1 \tilde{c}L, \quad (21)$$

while it is not too far from v_i , that is $|\tilde{v}_i - v_i| \leq \tilde{c}L$.

Proof The argument is volumetric. Let us first introduce the notation $U(X, r)$ for the set of all points $x \in \mathbb{R}^d$ such that $d(x, X) \leq r$, where X is any subset of \mathbb{R}^d . By definition of ρ_1 , see ‘Balls and exclusion volumes’ in Section 5.1, and because the dimension of $\text{span}(\tau'_j, T_p \mathcal{M})$ is at most $d-1$, we have that

$$\text{vol}(B(v_i, \tilde{c}L) \cap U(\text{span}(\tau'_j, T_p \mathcal{M}), \rho_1 \tilde{c}L)) \leq \frac{\text{vol}(B^d(r))}{2N_{\leq d-n-1}}.$$

It now follows that

$$\begin{aligned} & \text{vol} \left(B(v_i, \tilde{c}L) \setminus \left(\bigcup_{1 \leq j \leq v} U(\text{span}(\tau'_j, T_p \mathcal{M}), \rho_1 \tilde{c}L) \right) \right) \\ & \geq \text{vol}(B(v_i, \tilde{c}L)) - \sum_{0 \leq j \leq v} \text{vol}(B(v_i, \tilde{c}L) \cap U(\text{span}(\tau'_j, T_p \mathcal{M}), \rho_1 \tilde{c}L)) \\ & > \text{vol}(B(v_i, \tilde{c}L)) - \sum_{0 \leq j \leq v} \frac{\text{vol}(B(v_i, \tilde{c}L))}{2N_{\leq d-n-1}} \\ & = \text{vol}(B(v_i, \tilde{c}L)) \left(1 - \frac{v+1}{2N_{\leq d-n-1}} \right) \\ & \geq \frac{1}{2} \text{vol}(B(v_i, \tilde{c}L)), \end{aligned}$$

where we used that $v \leq N_{\leq d-n-1}$ in the last line, by definition, as mentioned in the description of Case 2. Because the volume is positive we know there exists a point \tilde{v}_i that satisfies

$$d(\tilde{v}_i, \text{span}(\tau'_j, T_p \mathcal{M})) > \rho_1 \tilde{c}L, \quad (22)$$

for all $1 \leq j \leq v$. □

The following lemma completes Case 2:

Lemma 22 *The triangulation $\tilde{\mathcal{T}}$ is $(d-n-1)$ -skeleton safe, in particular (16) is satisfied.*

Proof We first make use of the induction³ hypothesis $d(\tau'_j, \mathcal{M}) > \alpha_{k-1}L$ to find a bound on the distance from τ'_j to the tangent space $T_p \mathcal{M}$, then bound the distance from $\tilde{v}_i * \tau'_j = \tau_j$ to $T_p \mathcal{M}$ based on this. For this argument to work, we have to assume that τ'_j is not the empty set, that is $j \neq 0$. This case is handled separately at the end.

If we combine:

1. the induction hypothesis $d(\tau'_j, \mathcal{M}) > \alpha_{k-1}L$,
2. the fact that the ball in the tangent space $B_{T_p \mathcal{M}}(p, r)$ centred on p of radius $6L = r$, satisfies

$$B_{T_p \mathcal{M}}(p, r) \subset U \left(\mathcal{M}, \left(1 - \sqrt{1 - \left(\frac{r}{\text{rch}(\mathcal{M})} \right)^2} \right) \text{rch}(\mathcal{M}) \right),$$

thanks to Lemma 6,

we find that

$$d(\tau'_j, B_{T_p \mathcal{M}}(p, r)) > \alpha_{k-1}L - \left(1 - \sqrt{1 - \left(\frac{r}{\text{rch}(\mathcal{M})} \right)^2} \right) \text{rch}(\mathcal{M}).$$

This can be simplified:

$$\begin{aligned} & d(\tau'_j, B_{T_p \mathcal{M}}(p, r)) \\ & > \alpha_{k-1}L - \left(1 - \sqrt{1 - \left(\frac{r}{\text{rch}(\mathcal{M})} \right)^2} \right) \text{rch}(\mathcal{M}) \\ & > \alpha_{k-1}L - \frac{(\alpha_{d-n})^{4+2n}}{6(n+1)^2} \zeta^{2n} L && \text{(using (13))} \\ & > \alpha_{k-1}L - \frac{1}{3} \alpha_{d-n} L && \text{(using (15))} \\ & \geq \frac{2}{3} \alpha_{k-1} L. && \text{(because } \alpha_{k-1} > \alpha_k \text{)} \end{aligned} \tag{23}$$

Because $d(v_i, p) < \frac{3}{2}L$ and $\tilde{L} < L + 2\tilde{c}L$, and $\tilde{c} < \frac{1}{24}$, see (9), we have the very coarse bound that

$$d(\tau'_j, p) \leq 4L, \tag{24}$$

by the triangle inequality. We thus find that

$$d(\tau'_j, T_p \mathcal{M} \setminus B_{T_p \mathcal{M}}(p, r)) > 2L.$$

This means that (23) holds for the entire tangent space, that is,

$$d(\tau'_j, T_p \mathcal{M}) > \frac{2}{3} \alpha_{k-1} L. \tag{25}$$

³ In particular $\tau'_j \subset \tilde{\mathcal{F}}_i$.

Lemma 33, with $A_1 = T_p \mathcal{M}$ and $A_2 = \text{span}(\tau'_j, T_p \mathcal{M})$, now gives

$$d(\tau_j, T_p \mathcal{M}) \geq \frac{d(\tau'_j, T_p \mathcal{M})d(v_i, \text{span}(\tau'_j, T_p \mathcal{M}))}{L + 2\tilde{c}L}.$$

This can again be simplified

$$\begin{aligned} d(\tau_j, T_p \mathcal{M}) &\geq \frac{d(\tau'_j, T_p \mathcal{M})d(v_i, \text{span}(\tau'_j, T_p \mathcal{M}))}{L + 2\tilde{c}L} \\ &> \frac{\left(\frac{2}{3}\alpha_{k-1}L\right)\rho_1\tilde{c}L}{L + 2\tilde{c}L} && \text{(thanks to (25) and (21))} \\ &> \frac{\frac{2}{3}L}{\frac{4}{3}L}\alpha_{k-1}\rho_1\tilde{c}L && \text{(because } \tilde{c} \leq \frac{1}{24}\text{)} \\ &= \frac{4}{3}\alpha_k L. && \text{(using the relation (10) for } \alpha_k\text{)} \end{aligned} \tag{26}$$

Similarly to (24), we have that

$$d(\tau_j, p) \leq 4L < 6L.$$

We can go from the distance from τ_j to the tangent space, as given in (26), to the distance to the manifold as follows. Because of Corollary 5 we can localize the results and Lemma 6 allows us to estimate the difference in distance to the manifold and the tangent space. This gives

$$d(\tau_j, \mathcal{M}) > \frac{4}{3}\alpha_k L - \left(1 - \sqrt{1 - \left(\frac{6L}{\text{rch}(\mathcal{M})}\right)^2}\right) \text{rch}(\mathcal{M}).$$

This can be again simplified

$$\begin{aligned} d(\tau_j, \mathcal{M}) &> \frac{4}{3}\alpha_k L - \left(1 - \sqrt{1 - \left(\frac{6L}{\text{rch}(\mathcal{M})}\right)^2}\right) \text{rch}(\mathcal{M}) \\ &> \frac{4}{3}\alpha_k L - \frac{1}{3}\alpha_{d-n}L && \text{(using (13) and (15))} \\ &\geq \alpha_k L. && \text{(because } \alpha_k \geq \alpha_{d-n} \text{ if } k \leq d - n - 1 \text{ by (10))} \end{aligned}$$

This completes the proof for the case where $j \neq 0$ or τ_j is non-empty.

For $j = 0$, (22) and Lemma 6 yield

$$d(\tau_j, \mathcal{M}) > \rho_1 \tilde{c}L - \left(1 - \sqrt{1 - \left(\frac{6L}{\text{rch}(\mathcal{M})}\right)^2}\right) \text{rch}(\mathcal{M}).$$

We simplify

$$\begin{aligned}
d(\tau_j, \mathcal{M}) &> \rho_1 \tilde{c}L - \left(1 - \sqrt{1 - \left(\frac{6L}{\text{rch}(\mathcal{M})}\right)^2}\right) \text{rch}(\mathcal{M}). \\
&> \rho_1 \tilde{c}L - \frac{1}{3} \alpha_{d-n}L && \text{(using (13) and (15))} \\
&> \alpha_1 L. && \text{(by definition of (10))}
\end{aligned}$$

□

We emphasize that in the perturbation of the points it suffices to look at the tangent spaces at specific points, making this constructive proof an algorithm.

6 Constructing the triangulation of \mathcal{M}

Section 6.1 gives geometric consequences of the perturbation we discussed in the previous section. Most importantly we shall see that a simplex $\tilde{\sigma}$ in $\tilde{\mathcal{T}}$ intersects \mathcal{M} if and only if it intersects the tangent space $T_p \mathcal{M}$ of \mathcal{M} at a nearby point p close to σ , see Lemma 24. Here we again rely on Appendix B. The triangulation K of \mathcal{M} is defined in Section 6.2.

6.1 The geometry of the intersection of simplices in $\tilde{\mathcal{T}}$ and \mathcal{M}

In this section, we discuss the geometry of simplices in $\tilde{\mathcal{T}}$ in relation to \mathcal{M} . We follow [52, Section IV.19], with the usual exceptions of the use of Coxeter triangulations, the thickness, and the reach to quantify the results. The proofs also differ in a fair number of places from the original.

For any $p \in \mathcal{M}$ we first establish a lower bound on the distance between $T_p \mathcal{M}$ and simplices in the $(d-n-1)$ -skeleton of \mathcal{T} that are close to p .

Lemma 23 *Let $p \in \mathcal{M}$ and suppose that $\tau^k \in \tilde{\mathcal{T}}$, with $k \leq d-n-1$, such that $\tau^k \subset B(p, 6L)$, then*

$$d(\tau^k, T_p \mathcal{M}) > \frac{2}{3} \alpha_k L.$$

The following proof differs from Whitney's proof.

Proof of Lemma 23 Because $\tau^k \subset B(p, 6L)$, the point in $T_p \mathcal{M}$ that is closest to τ lies in $T_p \mathcal{M} \cap B(p, 6L) = B_{T_p \mathcal{M}}(p, 6L)$. We now see that

$$\begin{aligned}
d(\tau^k, T_p \mathcal{M}) &\geq d(\tau^k, B_{T_p \mathcal{M}}(p, 6L)) && \text{(first sentence of the proof)} \\
&> d(\tau^k, \mathcal{M}) - \left(1 - \sqrt{1 - \left(\frac{6L}{\text{rch}(\mathcal{M})}\right)^2}\right) \text{rch}(\mathcal{M}) && \text{(Lemma 6)} \\
&> \alpha_k L - \frac{1}{3} \alpha_{d-n} L, && (d(\tau^k, \mathcal{M}) > \alpha_k L \text{ and (15)}) \\
&> \frac{2}{3} \alpha_k L, && (\alpha_k \geq \alpha_{d-n} \text{ for } k \leq d-n)
\end{aligned}$$

which completes the proof. \square

We can now examine the relation between intersections with the manifold and nearby tangent spaces.

Lemma 24 *Suppose that \mathcal{M} intersects $\tau^k \in \tilde{\mathcal{T}}$. Let $p \in \mathcal{M}$, such that $\tau^k \subset B(p, 6L)$, then $T_p\mathcal{M}$ intersects τ^k .*

Proof Let $\bar{p} \in \mathcal{M} \cap \tau^k$. Lemma 3 (and (13), (15)) gives us that $\bar{p} \in \pi_p^{-1}(B_{T_p\mathcal{M}}(p, 6L))$, where we use the notation of Definition 4. Lemma 6 gives that

$$d(\bar{p}, T_p\mathcal{M}) \leq \left(1 - \sqrt{1 - \left(\frac{6L}{\text{rch}(\mathcal{M})}\right)^2}\right) \text{rch}(\mathcal{M}) < \frac{1}{3}\alpha_{d-n}L.$$

Let $\check{\tau} \subset \tau^k$ be the face of smallest dimension such that $d(\check{\tau}, T_p\mathcal{M}) \leq \frac{2}{3}\alpha_{d-n}L$. This face exists thanks to the triangle inequality. By Lemma 23 we have the $\dim(\check{\tau}) \geq d - n$. Lemma 32 implies that $\check{\tau}$ intersects $T_p\mathcal{M}$. The reason for this is the following; $\check{\tau}$ is the simplex of the smallest dimension such that $d(\check{\tau}, T_p\mathcal{M}) \leq \frac{2}{3}\alpha_k L$ meaning in particular that $d(\check{\tau}, T_p\mathcal{M}) < d(\partial\check{\tau}, T_p\mathcal{M})$. Because $\check{\tau}$ is a face of τ^k , clearly $T_p\mathcal{M}$ intersects τ^k . \square

We can now bound the angle between simplices and tangent spaces. In this case the proof identical to original, and included for completeness.

Lemma 25 *Suppose that \mathcal{M} intersects $\tau^k \in \tilde{\mathcal{T}}$ and τ^k has dimension $d - n$, that is $k = d - n$. Let $p \in \mathcal{M}$, such that $\tau^k \subset B(p, 6L)$, then*

$$\sin \angle(\text{aff}(\tau^k), T_p\mathcal{M}) \geq \frac{2d(T_p\mathcal{M}, \partial\tau^k)}{L + 2\tilde{c}L} \geq \frac{\frac{4}{3}\alpha_k L}{L + 2\tilde{c}L} \geq \frac{16}{13}\alpha_k.$$

Proof This is an immediate consequence of Lemma 32, (19), and the previous lemmas. \square

Below we investigate the relation between intersections of tangent spaces and simplices and intersections between the manifold and simplices. We combine two statements of Section IV.19 in the following lemma. The proof differs from the original by Whitney.

Lemma 26 *If $p \in \mathcal{M}$, $\tau^k \in \tilde{\mathcal{T}}$ and $\tau^k \subset B(p, 6L)$, and moreover $T_p\mathcal{M}$ intersects τ^k , then $k \geq d - n$ and \mathcal{M} intersects τ^k . If $k = d - n$ this point is unique, which in particular means that every simplex of dimension $d - n$ contains at most one point of \mathcal{M} .*

Proof Let $\check{\tau}$ be a face of smallest dimension of τ^k such that $d(\check{\tau}, T_p\mathcal{M}) \leq \frac{2}{3}\alpha_n L$. Now Lemma 32 and Lemma 24 give that $\check{\tau}$ and $T_p\mathcal{M}$ have a unique point \bar{p} in common and the dimension of $\check{\tau}$ is $d - n$.

Thanks to Lemma 3, \mathcal{M} can be written as the graph of a function f , in a neighbourhood of at most size $\text{rch}(\mathcal{M})$. We note that $f : T_p\mathcal{M} \simeq \mathbb{R}^n \rightarrow N_p\mathcal{M} \simeq \mathbb{R}^{d-n}$,

where here we really think of the tangent and normal spaces as embedded in \mathbb{R}^d . Using the identification of $T_p\mathcal{M}$ with \mathbb{R}^n , we now define

$$F : \mathbb{R} \times \mathbb{R}^n \rightarrow \mathbb{R}^d : (\lambda, x) \mapsto (x, \lambda f(x)).$$

Note that $F(0, \cdot)$ gives a parametrization of $T_p\mathcal{M}$. Similarly, we can define $G : \mathbb{R}^{d-n} \rightarrow \mathbb{R}^d$ to be a linear (orthonormal) parametrization of $\text{aff}(\check{\tau})$. We now consider the difference of the two functions $F - G : \mathbb{R} \times \mathbb{R}^n \times \mathbb{R}^{d-n} = \mathbb{R} \times \mathbb{R}^d \rightarrow \mathbb{R}^d$. Thanks to Lemma 25 we have that

$$\sin \angle(\text{aff}(\check{\tau}), T_p\mathcal{M}) \geq \frac{16}{13} \alpha_{d-n}.$$

Lemma 2, and (15) give that for any $q \in B(p, 6L)$

$$\sin \left(\frac{\angle(T_p\mathcal{M}, T_q\mathcal{M})}{2} \right) \leq \frac{6L}{2\text{rch}(\mathcal{M})} \leq \frac{6}{2} \cdot \frac{(\alpha_{d-n})^2}{54} = \frac{1}{18} (\alpha_{d-n})^2.$$

It is clear that this also gives an upper bound on the angle between $T_p\mathcal{M}$ and the graph of $F(\lambda, \cdot)$ (denoted by $\text{graph}F(\lambda, \cdot)$) for all $\lambda \in [0, 1]$, due to linearity of the inner product. Because the upper bound on the angle between the tangent spaces is much smaller than the lower bound on $\angle(\text{aff}(\tau^k), T_p\mathcal{M})$, $\text{aff}(\check{\tau})$ and the tangent space to the graph $T_q\text{graph}F(\lambda, \cdot)$ span \mathbb{R}^d , for any $\lambda \in [0, 1]$ and $q \in B(p, 6L)$. The implicit function theorem and the fact that $\check{\tau}$ and $T_p\mathcal{M}$ have a unique point \bar{p} in common now give that the intersection \bar{p}_λ between $\text{graph}F(\lambda, \cdot) \cap B(p, 6L)$ and $\text{aff}(\check{\tau})$ exists and is unique, for all $\lambda \in [0, 1]$.

We can now use Lemmas 3, 6, and 25, to bound $|\bar{p} - \bar{p}_\lambda|$. The distance from the manifold to the tangent space is bounded from above by

$$\frac{(\alpha_{d-n})^{3+2n}}{3(n+1)} \zeta^{2n} L < \frac{1}{3} (\alpha_{d-n})^2 L,$$

due to (13), and (15). The same bound holds for $\text{graph}F(\lambda, \cdot)$. We also have that $\sin \angle(\text{aff}(\check{\tau}), T_p\mathcal{M}) \geq \frac{16}{13} \alpha_{d-n}$. Combining these observations gives

$$|\bar{p} - \bar{p}_\lambda| \leq \frac{\frac{1}{3} (\alpha_{d-n})^2 L}{\frac{16}{13} \alpha_{d-n}} \leq \frac{1}{3} \alpha_{d-n} L.$$

This distance bound is smaller than the distance bound of \bar{p} to the boundary of $\check{\tau}$, due to Lemma 23. This means that $\bar{p}_\lambda \in \check{\tau}$, and in particular that \mathcal{M} intersects τ^k . \square

Finally, we study the faces of a simplex that intersects \mathcal{M} . This is essential for the barycentric subdivision in part 2 of the algorithm. The proof is identical to the original, but added for completeness.

Lemma 27 *If \mathcal{M} intersects $\tau = \{v_0, \dots, v_r\} \in \mathcal{T}$, then for each $v_i \in \tau$, there exists some $(d-n)$ -face τ' of τ such that $v_i \in \tau'$ and τ' intersects \mathcal{M} .*

Proof Take $p \in \mathcal{M} \cap \tau$. Let $\check{\tau}^k$ be a face of the smallest dimension of τ , with $v_i \in \check{\tau}^k$, that intersects $T_p \mathcal{M}$. Now assume that $k > d - n$. Let us write $\check{\tau}^{k-1}$ for the face of $\check{\tau}^k$ opposite v_i . Because the dimension of $\check{\tau}^k \cap T_p \mathcal{M}$ is at least 1, the intersection of $T_p \mathcal{M}$ and $\check{\tau}^{k-1}$ is non-empty.

Similarly to the first argument in the proof of Lemma 26, we see that $T_p \mathcal{M}$ intersects some $(d - n)$ -face of $\check{\tau}^{k-1}$. Thanks to Lemma 25, the angle between this $(d - n)$ -face and $T_p \mathcal{M}$ is bounded from below. Due to Lemma 23, the intersection lies in the interior of the $(d - n)$ -face. The angle bound and the fact that the intersection lies in the interior gives that any simplex in \mathcal{T} that contains this $(d - n)$ -face has points in the interior that lie in $T_p \mathcal{M}$. In particular the interior of $\check{\tau}^k$ contains part of $T_p \mathcal{M}$. Because both the interior of $\check{\tau}^k$ and $\check{\tau}^{k-1}$ contain points of $T_p \mathcal{M}$, linearity gives that $T_p \mathcal{M}$ must intersect $\partial \check{\tau}^k \setminus \check{\tau}^{k-1}$. From this contradiction of the assumption, we conclude that $k = d - n$.

Lemma 26 finally says that \mathcal{M} intersects $\check{\tau}^k$, because $T_p \mathcal{M}$ does. \square

6.2 The triangulation of \mathcal{M} : The complex K

The construction of the complex follows Section IV.20 of [52].

In each simplex τ of $\tilde{\mathcal{T}}$ that intersects \mathcal{M} , we choose a point $v(\tau)$ and construct a complex K with these points as vertices. The construction goes via barycentric subdivision of general polytopes or even CW-complexes, see for example [40, Theorem 1.7 of Chapter III]. For each sequence $\tau_0 \subset \tau_1 \subset \dots \subset \tau_k$ of distinct simplices in $\tilde{\mathcal{T}}$ such that τ_0 intersects \mathcal{M} ,

$$\sigma^k = \{v(\tau_0), \dots, v(\tau_k)\} \quad (27)$$

will be a simplex of K . The definition of $v(\tau)$ depends on the dimension of τ :

- If τ is a simplex of dimension $d - n$, then there is an unique point of intersection with \mathcal{M} , due to Lemma 26. We define $v(\tau)$ to be this unique point.
- If τ has dimension greater than $d - n$, then we consider the faces $\tau_1^{d-n}, \dots, \tau_j^{d-n}$ of τ of dimension $d - n$ that intersect \mathcal{M} . These faces exist thanks to Lemma 27. We now define $v(\tau)$ as follows:

$$v(\tau) = \frac{1}{j} \left(v(\tau_1^{d-n}) + \dots + v(\tau_j^{d-n}) \right). \quad (28)$$

Remark 3 We stress that thanks to Lemma 26, choosing the point $v(\tau^{d-n})$ to be the point of intersection with $T_p \mathcal{M}$, assuming p is sufficiently close, locally gives the same combinatorial structure as intersections with \mathcal{M} . We also stress that for the combinatorial structure it does not really matter where \mathcal{M} intersects a simplex of $\tilde{\mathcal{T}}$, as long as it does.

We can now state the following bound on the altitudes of the simplices we constructed in this manner.

Lemma 28 *Let σ^n be a top dimensional simplex as defined in (27), then*

$$\min \text{alt}(\sigma^n) > \zeta^n (\alpha_{d-n-1})^n \tilde{L},$$

where $\min \text{alt}$ denotes the minimal altitude or height, and we used the notation ζ , as defined in (12).

Proof This inequality relies on estimates on the barycentric coordinates, and Lemma 12. We first establish a bound on the barycentric coordinates of $v(\tau_i^{d-n})$ for some $(d-n)$ -dimensional simplex $\tau_i^{d-n} \in \tilde{\mathcal{T}}$ that intersects \mathcal{M} . By Lemma 23, $v(\tau_i^{d-n})$ lies at least a distance $\frac{2}{3}\alpha_{d-n-1}L$ from the boundary $\partial\tau_i^{d-n}$, and the longest edge is at most $L + 2\tilde{c}L$. This means that all the barycentric coordinates λ_l with respect to (the vertices of) τ_i^{d-n} are at least

$$\lambda_l(\tau_i^{d-n}) > \frac{2}{3}\alpha_{d-n-1}\frac{L}{L+2\tilde{c}L} = \frac{2}{3}\alpha_{d-n-1}\frac{1}{1+2\tilde{c}}. \quad (29)$$

Let τ^d now be a top dimensional simplex in $\tilde{\mathcal{T}}$ that intersects \mathcal{M} . Let $\tau_1^{d-n}, \dots, \tau_j^{d-n}$ be the faces of τ^d that intersect \mathcal{M} . This means that $d-n+1$ barycentric coordinates with respect to τ^d of any $v(\tau_i^{d-n})$ satisfy the bound (29), while the other n coordinates are zero. This also means that for the barycentric coordinates with respect to τ^d of

$$v(\tau^k) = \frac{1}{j} \left(v(\tau_1^{d-n}) + \dots + v(\tau_j^{d-n}) \right),$$

for $k > d-n$, we have that

- $k+1$ of the coordinates λ_l satisfy

$$\lambda_l > \frac{2}{3}\frac{1}{j}\frac{1}{1+2\tilde{c}}\alpha_{d-n-1}.$$

- The other $d-k$ coordinates are zero.

Note that $j \leq \binom{d}{d-n}$. This means that

$$d(v(\tau^k), \partial\tau^k) \geq \frac{2}{3\binom{d}{d-n} \cdot (1+2\tilde{c})} \alpha_{d-n-1} \min \text{alt}(\tau^d).$$

We now have

$$\begin{aligned} d(v(\tau^k), \partial\tau^k) &\geq \frac{2}{3\binom{d}{d-n} \cdot (1+2\tilde{c})} \alpha_{d-n-1} t(\tilde{\mathcal{T}}) \tilde{L} \quad (\text{by definition of the thickness}) \\ &\geq \frac{2}{3\binom{d}{d-n} \cdot (1+2\tilde{c})} \alpha_{d-n-1} \frac{4}{5\sqrt{d}} \left(1 - \frac{8\tilde{c}}{t(\mathcal{T})^2} \right) t(\mathcal{T}) \tilde{L} \\ &\hspace{15em} (\text{by the estimate (18)}) \\ &\geq \frac{8}{15\sqrt{d} \binom{d}{d-n} \cdot (1+2\tilde{c})} \left(1 - \frac{8\tilde{c}}{t(\mathcal{T})^2} \right) \alpha_{d-n-1} t(\mathcal{T}) \tilde{L} \quad (30) \end{aligned}$$

Using this estimate and the fact that σ^n is defined through a sequence $\tau_0^{d-n} \subset \tau_1^{d-n+1} \subset \dots \subset \tau_n^d$, we can give a lower bound on the minimal altitude of the simplex.

We are going to use the following easy observation on the minimal altitude simplices. Suppose that:

- The simplex σ is the join of a point p and the simplex σ' .
- $d(p, \text{aff}(\sigma')) \geq d_{\min}$.
- $\min \text{alt}(\sigma') \geq h'$.
- The maximum edge length of σ is $L(\sigma)$.

Then the $\min \text{alt}(\sigma) \geq \frac{h' d_{\min}}{L(\sigma)}$, as can be established by simple trigonometric arguments, as illustrated in Figure 5. Applying this result n times gives that

$$\begin{aligned} \min \text{alt}(\sigma^n) &\geq \frac{h(\sigma^{n-1}) d_{\min}(\sigma^n)}{L(\sigma^n)} \\ &\geq \frac{h(\sigma^{n-2}) d_{\min}(\sigma^n) d_{\min}(\sigma^{n-1})}{L(\sigma^n)^2} \\ &\geq \frac{d_{\min}(\sigma^n) \dots d_{\min}(\sigma^0)}{L(\sigma^n)^n}, \end{aligned} \quad (31)$$

where we indicated the dimensions explicitly.

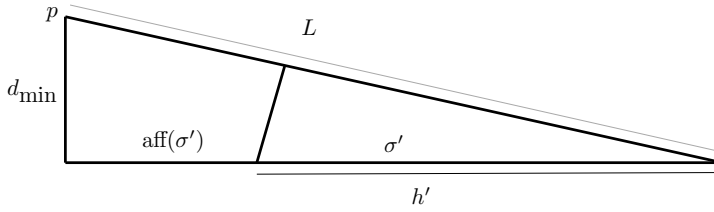


Fig. 5 Both triangles are right angled. We stress that the projection of p onto $\text{aff}(\sigma')$ may be quite a distance from σ' itself.

Plugging (30) (using the definition of the simplex σ^n as in (27)) into (31) gives that $\min \text{alt}(\sigma^n)$ is lower bounded as follows:

$$\begin{aligned} \min \text{alt}(\sigma^n) &> \left(\frac{8}{15\sqrt{d} \binom{d}{d-n} \cdot (1+2\tilde{c})} \left(1 - \frac{8\tilde{c}}{t(\mathcal{T})^2} \right) \alpha_{d-n-1} t(\mathcal{T}) \right)^n \tilde{L} \\ &= \zeta^n (\alpha_{d-n-1})^n \tilde{L}, \end{aligned}$$

which completes the proof. \square

7 The triangulation proof

Given the triangulation $\tilde{\mathcal{T}}$, we want to prove that the intersection of $\mathcal{M} \cap \tau^d$ is homeomorphic to the triangulated polytope described in Section 6.2. This immediately gives a global homeomorphism between the triangulation and the manifold.

The homeomorphism we discuss in this section differs greatly from Whitney's own approach. Firstly, he used the closest point projection as a map (which does not respect simplices, meaning that the point in the complex K (as defined in the previous

section) and its projection may lie in different simplices of $\tilde{\mathcal{T}}$. Secondly, to prove that this map is a homeomorphism, he uses what has become known as Whitney's lemma in much the same way as in [15].

The great advantage of our approach to the homeomorphism proof is that it is extremely explicit and it is elementary in the sense that it does not rely on topological results. We also need precise bounds on the angles, which do not require deep theory, but are quite intricate.

Because we work with an ambient triangulation of type \tilde{A} and we do not perturb too much, the simplices of $\tilde{\mathcal{T}}$ are Delaunay. The homeomorphism from $\mathcal{M} \cap \tau^d$ to the triangulated polytope $K \cap \tau^d$, with K as defined in Section 6.2 and $\tau^d \in \tilde{\mathcal{T}}$, gives that the intersection of any simplex in $\tilde{\mathcal{T}}$ with \mathcal{M} is a topological ball of the appropriate dimension. This may remind the reader of the closed ball property of Edelsbrunner and Shah [35]. We stress that the homeomorphism we construct is explicit.

Overall homeomorphism proof. The homeomorphism proof consists of three steps:

- For each d -simplex $\tau \in \tilde{\mathcal{T}}$ we provide a ‘tubular neighbourhood’ for $K \cap \tau$ adapted to τ . By this we mean that, for each point \bar{p} in $K \cap \tau$, we designate a ‘normal’ space $\mathcal{N}_{\bar{p}}$ that has dimension equal to the codimension of \mathcal{M} and K and is transversal to $K \cap \tau$. Moreover, these directions shall be chosen in a sufficiently controlled and smooth way, so that every point x in τ that is sufficiently close to K has a unique point \bar{p} on $K \cap \tau$ such that $x - \bar{p} \in \mathcal{N}_{\bar{p}}$.
- We give conditions that enforce that the ‘normal’ spaces $\mathcal{N}_{\bar{p}}$ intersect \mathcal{M} transversely. More precisely, we prove that the angle between $\tilde{\mathcal{N}}_{\bar{p}}$ and $N_q \mathcal{M}$, for any $q \in \mathcal{M} \cap \tau$ is upper bounded by a quantity strictly less than 90 degrees.
- We conclude that the projection along $\mathcal{N}_{\bar{p}}$ gives a homeomorphism from \mathcal{M} to K .

7.1 Constructing the tubular neighbourhood

We now give the construction of the ‘tubular neighbourhood’ of K . We use two results from the previous sections:

- The normal space is almost constant, see Lemma 2, near a simplex $\tau \in \tilde{\mathcal{T}}$, because it is small. So $T\mathcal{M}$ and $N\mathcal{M}$ near p are well approximated by $T_p\mathcal{M}$ and $N_p\mathcal{M}$.
- The angles between the normal space and faces $\tau_1^{d-n}, \dots, \tau_j^{d-n}$ of τ of dimension $d - n$ that intersect \mathcal{M} are bounded from below by Lemma 25.

As a consequence the orthogonal projection map $\pi_{\text{aff}(\tau_k^{d-n}) \rightarrow N_p\mathcal{M}} \equiv \pi_{\tau_k^{d-n}}$ from the affine hull $\text{aff}(\tau_k^{d-n})$ to $N_p\mathcal{M}$ is a (linear) bijection, for any p that is sufficiently close to τ_k^{d-n} , with $k \in \{1, \dots, j\}$. We will denote the inverse of this map by $\pi_{\tau_k^{d-n}}^{-1}$.

We can now define the ‘normal spaces’ for the complex K . We first do this for the vertices $v(\tau)$, where τ has dimension $d - n$ (these vertices lie on \mathcal{M}), secondly for general vertices of K (these vertices do not necessarily lie on \mathcal{M}) and finally using barycentric coordinates for arbitrary points in K .

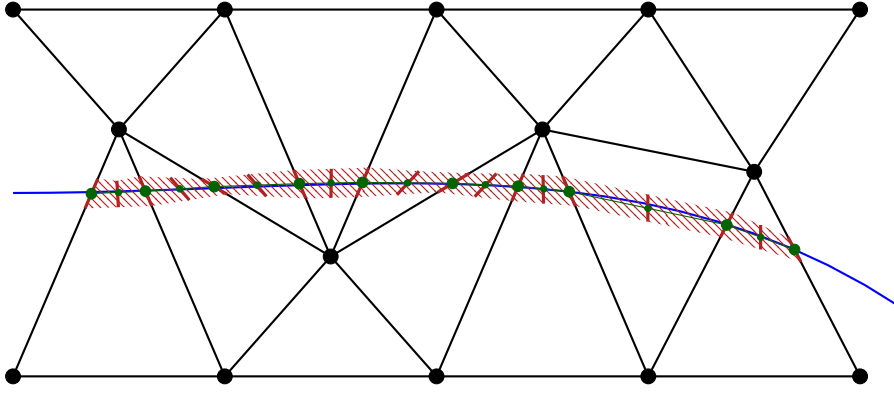


Fig. 6 The tubular neighbourhood.

We start, as mentioned, with the vertices that are associated to a simplex $\tau = \tau^{d-n} \in \tilde{\mathcal{F}}$ of dimension $d-n$. We stress that there is but one face of dimension $d-n$ of τ , namely itself, so $\tau = \tau^{d-n} = \tau_1^{d-n}$. For the vertex $v(\tau) = v(\tau^{d-n}) = v(\tau_1^{d-n})$ we choose the normal space $\mathcal{N}_{v(\tau_1^{d-n})}$ to be $\text{aff}(\tau_1^{d-n})$.

For $v(\tau)$, such that the dimension of τ is greater than $d-n$ we make the following construction, which is reminiscent of the construction of $v(\tau)$ in Section 6.2. Let $p \in \mathcal{M}$ be such that $\tau \subset B(p, 6L)$. For now p is arbitrary, we'll specify this later. We consider the faces $\tau_1^{d-n}, \dots, \tau_j^{d-n}$ of τ of dimension $d-n$ that intersect \mathcal{M} . Now consider the orthogonal projection map $\pi_{v(\tau_k^{d-n}), p} : \text{aff}(\tau_k^{d-n}) \rightarrow N_p \mathcal{M}$. For any $w \in N_p \mathcal{M}$, we define

$$N_{\tau, p}(w) = \frac{1}{j} \left(\pi_{v(\tau_1^{d-n}), p}^{-1}(w) + \dots + \pi_{v(\tau_j^{d-n}), p}^{-1}(w) \right). \quad (32)$$

To construct the normal space at $v(\tau)$, we pick $p = \pi_{\mathcal{M}}(v(\tau))$ and define the normal space as $\mathcal{N}_{v(\tau)} = \text{span}(N_{\tau, \pi_{\mathcal{M}}(v(\tau))}(w))$.

Let $\sigma^n = \{v(\tau_0^{d-n}), \dots, v(\tau_n^d)\}$ be a simplex of K . Now choose a point $p \in \mathcal{M}$ as before. For any point \bar{p} in σ^n with barycentric coordinates $\lambda = (\lambda_0, \dots, \lambda_n)$, and any $w \in N_p \mathcal{M}$ we define

$$N_{\bar{p}, p}(w) = \lambda_0 N_{\tau_0^{d-n}, p}(w) + \dots + \lambda_n N_{\tau_n^d, p}(w). \quad (33)$$

We now set $p = \pi_{\mathcal{M}}(\bar{p})$. By defining $\mathcal{N}_{\bar{p}} = \text{span}(N_{\bar{p}, \pi_{\mathcal{M}}(\bar{p})}(w))$, we get affine spaces for each point in each $\sigma^n \in K$.

Remark 4 By construction, these spaces are consistent on the faces of simplices in K as well as with the boundaries of the d dimensional simplices in $\tilde{\mathcal{F}}$.

The tubular neighbourhood is defined as the set of all points in \mathbb{R}^d that that lie in a unique $\mathcal{N}_{\bar{p}}$, with $p \in K$.

7.2 The size of the tubular neighbourhoods and the homeomorphism

In this section, we establish the size of the neighbourhood of K as defined by $\mathcal{N}_{\bar{p}}$.

The following angle estimate is an essential part of the estimate of the size of the neighbourhood of the triangulation K .

Lemma 29 *Suppose that $p \in \mathcal{M}$, $\tau^d \subset B(p, 6L)$ and $\sigma^n \in K$ such that $\sigma^n \subset \tau^d$, where we regard σ^n and τ^d as subsets of \mathbb{R}^d . Then the angle between $T_p \mathcal{M}$ and $\text{aff}(\sigma^n)$ is bounded as follows:*

$$\sin \angle(\text{aff}(\sigma^n), T_p \mathcal{M}) \leq \frac{(\alpha_{d-n})^{4+n}}{6(n+1)} \zeta^n.$$

Proof By Lemma 13, we have

$$\sin \angle(\text{aff}(\sigma^n), T_p \mathcal{M}) \leq \frac{(n+1)d_{\max}}{\min \text{alt}(\sigma^n)},$$

where d_{\max} denotes the maximum distance of the vertices of σ^n to $T_p \mathcal{M}$. Lemma 28 gives us the following bound

$$\min \text{alt}(\sigma^n) > (\alpha_{d-n-1})^n \zeta^n \tilde{L}.$$

Finally, d_{\max} is bounded thanks to (13). Combining these results yields

$$\begin{aligned} \sin \angle(\text{aff}(\sigma^n), T_p \mathcal{M}) &\leq \frac{(n+1) \frac{(\alpha_{d-n})^{4+2n}}{6(n+1)^2} \zeta^{2n} L}{(\alpha_{d-n-1})^n \zeta^n \tilde{L}} \\ &\leq \frac{(\alpha_{d-n})^{4+n}}{6(n+1)} \zeta^n. \end{aligned}$$

(because $\alpha_{d-n-1} < \alpha_{d-n}$, and $\tilde{L} \geq L$ because there are unperturbed simplices in $\tilde{\mathcal{T}}$)

□

With this we can give a bound on the size of the neighbourhood of K .

Lemma 30 *Let $\bar{p}, \bar{q} \in \sigma^n$, with barycentric coordinates $\lambda = (\lambda_0, \dots, \lambda_n)$, $\lambda' = (\lambda'_0, \dots, \lambda'_n)$ respectively. Suppose that $\mathcal{N}_{\bar{p}}$ and $\mathcal{N}_{\bar{q}}$ be as defined in Section 7.1. Suppose now that the intersection between $\bar{p} + \mathcal{N}_{\bar{p}}$ and $\bar{q} + \mathcal{N}_{\bar{q}}$ is non-empty. Here $\bar{p} + \mathcal{N}_{\bar{p}}$ and $\bar{q} + \mathcal{N}_{\bar{q}}$ denote the affine spaces that go through \bar{p} , \bar{q} and are parallel to $\mathcal{N}_{\bar{p}}$, $\mathcal{N}_{\bar{q}}$, respectively. If $x \in \bar{p} + \mathcal{N}_{\bar{p}} \cap \bar{q} + \mathcal{N}_{\bar{q}}$, then*

$$d(x, \text{aff}(\sigma^n)) \geq \frac{\left(\frac{15}{13}\right)^2 (\alpha_{d-n})^4}{n+1} \zeta^n (\alpha_{d-n-1})^n \tilde{L}. \quad (34)$$

Because, by construction, the $\mathcal{N}_{\bar{p}}$ agree on the faces of the n -dimensional simplices in K , this provides a tubular neighbourhood for K of the size indicated in the right hand side of (34).

Proof The main idea of the proof of this lemma is the following: Given two points $\bar{p}, \bar{q} \in \sigma^n \subset K$ the ‘normal’ spaces $\mathcal{N}_{\bar{p}}$ and $\mathcal{N}_{\bar{q}}$ do not intersect too close to K , if the angle between $\mathcal{N}_{\bar{p}}$ and $\mathcal{N}_{\bar{q}}$ is not too large compared to the distance between \bar{p} and \bar{q} (and the angle between $\mathcal{N}_{\bar{p}}$ and $\text{aff}(\sigma)$ is not too small). The proof consists of several steps. Step 0, gives some very rough estimates, mainly on the angles between the various ‘normal’ spaces of K that we construct and $N_{p \cdot \mathcal{M}}$. Steps 1, 2, and 3 work from these very naive bounds to fairly sharp estimates on $\angle(\mathcal{N}_{\bar{p}}, \mathcal{N}_{\bar{q}})$. In the fourth and final step the bound on $\angle(\mathcal{N}_{\bar{p}}, \mathcal{N}_{\bar{q}})$ is used to give a lower bound on the size of the tubular neighbourhood.

Step 0: preliminary estimates

Lemma 25 gives that for each τ^{d-n}

$$\sin \angle(\text{aff}(\tau^{d-n}), T_{p \cdot \mathcal{M}}) \geq \frac{16}{13} \alpha_{d-n},$$

or,

$$\cos \angle(\text{aff}(\tau^{d-n}), N_{p \cdot \mathcal{M}}) \geq \frac{16}{13} \alpha_{d-n},$$

so that for $u \in N_{p \cdot \mathcal{M}}$ of unit length,

$$\cos \angle(\pi_{v(\tau_k^{d-n}), p}^{-1}(u), u) \geq \frac{16}{13} \alpha_{d-n},$$

with $\pi_{v(\tau_k^{d-n}), p} : \text{aff}(\tau_k^{d-n}) \rightarrow N_{p \cdot \mathcal{M}}$ the orthogonal projection map.

This means that $|\pi_{v(\tau_k^{d-n}), p}^{-1}(u)| \leq \frac{13}{16\alpha_{d-n}}$. Together with the triangle inequality this yields that

$$|N_{\tau, p}(u)|, |N_{\bar{p}}(u')| \leq \frac{13}{16\alpha_{d-n}}, \quad (35)$$

for any $u \in N_{p \cdot \mathcal{M}}$ and $u' \in N_{\pi_{\mathcal{M}}(\bar{p}) \cdot \mathcal{M}}$ of unit length. By construction the component of $N_{\tau, p}(u)$ in the u direction is u and the component of $N_{\bar{p}}(u')$ in the u' direction is also u' . This in turn gives us that

$$\angle(N_{\tau, p}(u), u), \angle(N_{\bar{p}}(u'), u') \leq \arccos\left(\frac{16}{13} \alpha_{d-n}\right). \quad (36)$$

Thus

$$\angle\left(\text{span}_{u \in N_{p \cdot \mathcal{M}}}(N_{\tau, p}(u)), N_{p \cdot \mathcal{M}}\right), \angle(\mathcal{N}_{\bar{p}}, N_{\pi_{\mathcal{M}}(\bar{p}) \cdot \mathcal{M}}) \leq \arccos\left(\frac{16}{13} \alpha_{d-n}\right). \quad (37)$$

If we want to compare the two different normal spaces $N_{p \cdot \mathcal{M}}$ and $N_{q \cdot \mathcal{M}}$, with $|p - q| \leq 4L$, we again invoke Lemma 2, and (15) to see that

$$\sin\left(\frac{\angle(N_{p \cdot \mathcal{M}}, N_{q \cdot \mathcal{M}})}{2}\right) \leq \frac{2L}{\text{rch}(\mathcal{M})} < \frac{(\alpha_{d-n})^{4+2n}}{29(n+1)^2} \zeta^n.$$

Using (11) and that ζ is small, we can further simplify

$$\sin\left(\frac{\angle(N_p \mathcal{M}, N_q \mathcal{M})}{2}\right) < \frac{\alpha_{d-n}}{18^3 * 29} = \frac{\alpha_{d-n}}{169128}$$

The triangle inequality for angles (or points on the sphere) now implies that

$$\begin{aligned} \angle\left(\underset{u \in N_p \mathcal{M}}{\text{span}}(N_{\tau,p}(u)), \underset{u \in N_q \mathcal{M}}{\text{span}}(N_{\tau,q}(u)), \angle(\mathcal{N}_{\bar{p}}, \mathcal{N}_{\bar{q}})\right) \\ < 2 \arccos\left(\frac{16}{13} \alpha_{d-n}\right) + \arcsin\left(\frac{\alpha_{d-n}}{18^3 * 29}\right). \end{aligned}$$

Overview steps 1, 2, and 3: angle estimates

Having established some preliminary estimates, we will tighten this result for $\angle(\mathcal{N}_{\bar{p}}, \mathcal{N}_{\bar{q}})$. The angle between these two terms is determined by both p and \bar{p} in $N_{\bar{p},p}(u)$. We will examine the effects of both separately.

Step 1: Bounding $\angle(N_{\bar{p},p}(u), N_{\bar{q},p}(u))$ We start by fixing p and varying \bar{p} . We now consider

$$N_{\bar{p},p}(u) = \lambda_0 N_{\tau_0^{d-n},p}(u) + \dots + \lambda_n N_{\tau_n^d,p}(u),$$

and

$$N_{\bar{q},p}(u) = \lambda'_0 N_{\tau_0^{d-n},p}(u) + \dots + \lambda'_n N_{\tau_n^d,p}(u).$$

We are now going to estimate the angle between these vectors and thus the angle between $\text{span}_u(N_{\bar{p},p}(u))$ and $\text{span}_u(N_{\bar{q},p}(u))$ in terms of the barycentric coordinates. The u components of $N_{\bar{p},p}(u)$ and $N_{\bar{q},p}(u)$ are u by construction as we mentioned before. We are going to compare this with the length of $N_{\bar{p},p}(u)$ and $N_{\bar{q},p}(u)$ and the length of their difference. For estimates on these lengths we need to introduce the following notation:

- $(N_{\tau_0^{d-n},p}(u) \dots N_{\tau_n^d,p}(u))$ denotes the matrix whose columns are $N_{\tau_0^{d-n},p}(u), \dots, N_{\tau_n^d,p}(u)$
- $\|\cdot\|_2$ denotes the operator 2-norm,
- $\|\cdot\|_F$ the Frobenius norm.

With this notation, we can now derive the following bound:

$$\begin{aligned}
& |\lambda_0 N_{\tau_0^{d-n},p}(u) + \cdots + \lambda_n N_{\tau_n^d,p}(u) - (\lambda'_0 N_{\tau_0^{d-n},p}(u) + \cdots + \lambda'_n N_{\tau_n^d,p}(u))| \\
&= |(\lambda_0 - \lambda'_0) N_{\tau_0^{d-n},p}(u) + \cdots + (\lambda_n - \lambda'_n) N_{\tau_n^d,p}(u)| \\
&= \left| (N_{\tau_0^{d-n},p}(u) \cdots N_{\tau_n^d,p}(u)) \begin{pmatrix} \lambda_0 - \lambda'_0 \\ \vdots \\ \lambda_n - \lambda'_n \end{pmatrix} \right| \\
&\leq \| (N_{\tau_0^{d-n},p}(u) \cdots N_{\tau_n^d,p}(u)) \|_2 |\lambda - \lambda'| \\
&\leq \| (N_{\tau_0^{d-n},p}(u) \cdots N_{\tau_n^d,p}(u)) \|_F |\lambda - \lambda'| \quad (\text{because } \|\cdot\|_2 \leq \|\cdot\|_F) \\
&= \sqrt{|N_{\tau_0^{d-n},p}(u)|^2 + \cdots + |N_{\tau_n^d,p}(u)|^2} |\lambda - \lambda'| \\
&\quad (\text{by definition of the Frobenius norm}) \\
&\leq \frac{13\sqrt{n+1}}{16\alpha_{d-n}} |\lambda - \lambda'|. \quad (\text{by (35)})
\end{aligned} \tag{38}$$

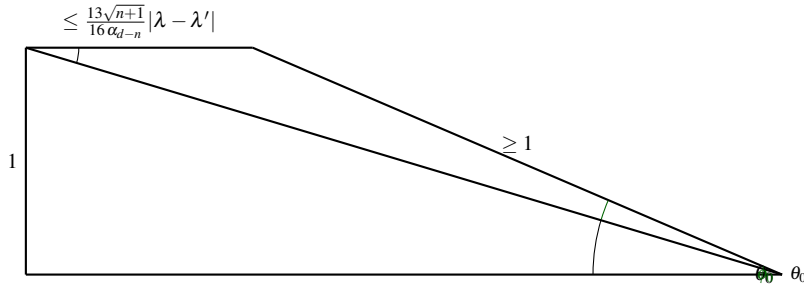


Fig. 7 The worst case for the angle between the vectors $N_{\bar{p}}(e_j)$ and $N_{\bar{q}}(e_j)$. We write ϕ_0 for an upper bound on $\angle(N_{\bar{p}}(e_j), N_{\bar{q}}(e_j))$. Moreover $\theta_0 \geq \arcsin(\frac{13}{16}\alpha_{d-n})$. The length or bound on the length of two of the edges is also indicated in the figure.

We now turn our attention to the triangle, with edges $N_{\bar{p},p}(u)$, $N_{\bar{q},p}(u)$, and $N_{\bar{p},p}(u) - N_{\bar{q},p}(u)$ as depicted in Figure 7. We apply the sine rule to this triangle, using (36), and (38), to find

$$\sin \angle(N_{\bar{p},p}(u), N_{\bar{q},p}(u)) \leq \sin \phi_0 = \frac{\frac{13\sqrt{n+1}}{16\alpha_{d-n}} |\lambda - \lambda'| \frac{13}{16\alpha_{d-n}}}{1} = \left(\frac{13}{16\alpha_{d-n}} \right)^2 \sqrt{n+1} |\lambda - \lambda'|. \tag{39}$$

Note that this can be tightened a fair bit at the cost of complicating the bound.

We conclude from (39) that

$$\sin \angle(\text{span}_u(N_{\bar{p},p}(u)), \text{span}_u(N_{\bar{q},p}(u))) \leq \left(\frac{13}{16\alpha_{d-n}} \right)^2 \sqrt{n+1} |\lambda - \lambda'|. \quad (40)$$

Step 2: bounding $\angle(\text{span}_{u \in N_{p,\mathcal{M}}}(N_{\bar{p},p}(u)), \text{span}_{u \in N_{q,\mathcal{M}}}(N_{\bar{p},q}(u)))$.

We now want to bound the angle between $\text{span}_{u \in N_{p,\mathcal{M}}}(N_{\bar{p},p}(u))$, $\text{span}_{u \in N_{q,\mathcal{M}}}(N_{\bar{p},q}(u))$ based on the distance between the points p and q in \mathcal{M} . We use that p and q are such that $\tau \subset B(p, 6L), B(q, 6L)$ so that the conditions of Lemma 25 hold. This also means that p and q are close, which means that the angle between $N_{q,\mathcal{M}}$ and $N_{p,\mathcal{M}}$ is very small. This gives that the projection $\pi_{N_{q,\mathcal{M}} \rightarrow N_{p,\mathcal{M}}}$ induces a (linear) bijection from $N_{q,\mathcal{M}}$ to $N_{p,\mathcal{M}}$, so that the inverse $\pi_{N_{q,\mathcal{M}} \rightarrow N_{p,\mathcal{M}}}^{-1}$ makes sense. Having established this map, we see that

$$\angle(\text{span}_{u \in N_{p,\mathcal{M}}}(N_{\bar{p},p}(u)), \text{span}_{u \in N_{q,\mathcal{M}}}(N_{\bar{p},q}(u))) \leq \sup_{u \in N_{p,\mathcal{M}}} \angle(N_{\bar{p},p}(u), N_{\bar{p},q}(\pi_{N_{q,\mathcal{M}} \rightarrow N_{p,\mathcal{M}}}^{-1}(u))) \quad (41)$$

To bound this angle, we look at the individual terms in (32), that is $\pi_{v(\tau_k^{d-n}),p}^{-1}(u)$ and $\pi_{v(\tau_1^{d-n}),q}^{-1}(\pi_{N_{q,\mathcal{M}} \rightarrow N_{p,\mathcal{M}}}^{-1}(u))$. See Figure 8 for an illustration. We can write $\pi_{N_{q,\mathcal{M}} \rightarrow N_{p,\mathcal{M}}}^{-1}(u) = u + \bar{w}_{q,p}$, with $\bar{w}_{q,p} \in T_{p,\mathcal{M}}$, $|\bar{w}_{q,p}| \leq \tan \angle(N_{p,\mathcal{M}}, N_{q,\mathcal{M}})$, and

$$|u + \bar{w}_{q,p}| \leq 1 / \cos \angle(N_{p,\mathcal{M}}, N_{q,\mathcal{M}}).$$

Similarly, $\pi_{v(\tau_k^{d-n}),p}^{-1}(u)$ can be written as $u + \bar{w}_{k,p}$, with $\bar{w}_{k,p} \in T_{p,\mathcal{M}}$, and

$$|\bar{w}_{k,p}| \leq \tan \angle(\text{aff}(\tau_k^{d-n}), N_{p,\mathcal{M}}).$$

Likewise, $\pi_{v(\tau_k^{d-n}),q}^{-1}(u + \bar{w}_{q,p})$ can be written as $u + \bar{w}_{q,p} + \bar{w}_{k,q}$, with $\bar{w}_{k,q} \in T_{q,\mathcal{M}}$, and

$$|\bar{w}_{k,q}| \leq \frac{\tan \angle(\text{aff}(\tau_k^{d-n}), N_{q,\mathcal{M}})}{\cos \angle(N_{p,\mathcal{M}}, N_{q,\mathcal{M}})}.$$

The distance from $\pi_{v(\tau_k^{d-n}),q}^{-1}(u + \bar{w}_{q,p})$ to the translation of $T_{p,\mathcal{M}}$ that goes through u is at most

$$\frac{\tan \angle(\text{aff}(\tau_k^{d-n}), N_{q,\mathcal{M}}) \sin \angle(T_{p,\mathcal{M}}, T_{q,\mathcal{M}})}{\cos \angle(N_{p,\mathcal{M}}, N_{q,\mathcal{M}})} = \frac{\tan \angle(\text{aff}(\tau_k^{d-n}), N_{q,\mathcal{M}}) \sin \angle(N_{p,\mathcal{M}}, N_{q,\mathcal{M}})}{\cos \angle(N_{p,\mathcal{M}}, N_{q,\mathcal{M}})}$$

By definition of the projection map $\pi_{v(\tau_k^{d-n}),p}$ the point $\pi_{v(\tau_k^{d-n}),p}^{-1}(u)$ lies in the translation of $T_{p,\mathcal{M}}$ that goes through u . Because also by definition $\pi_{v(\tau_k^{d-n}),p}^{-1}(u)$ and

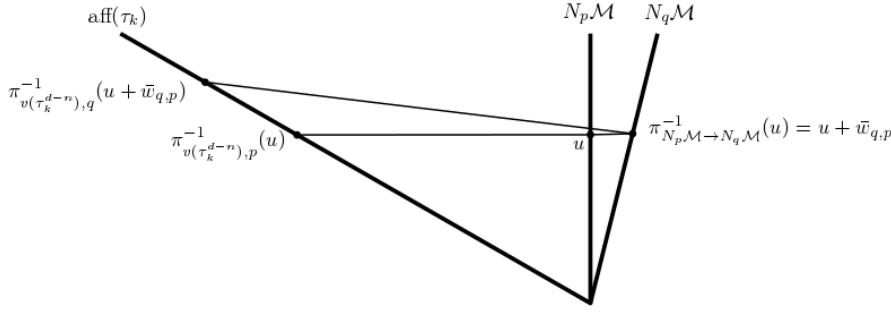


Fig. 8 Note that the two dimensional nature of the figure is slightly misleading.

$\pi_{v(\tau_k^{d-n}),q}^{-1}(u + \bar{w}_{q,p}) = \pi_{N_q\mathcal{M} \rightarrow N_p\mathcal{M}}^{-1}(u)$ are both contained in $\text{aff}(\tau_k^{d-n})$, we have that,

$$\begin{aligned}
 |\pi_{v(\tau_k^{d-n}),p}^{-1}(u) - \pi_{v(\tau_k^{d-n}),q}^{-1}(u + \bar{w}_{q,p})| &= |\pi_{v(\tau_k^{d-n}),p}^{-1}(u) - \pi_{v(\tau_k^{d-n}),q}^{-1}(\pi_{N_q\mathcal{M} \rightarrow N_p\mathcal{M}}^{-1}(u))| \\
 &\leq \frac{\tan \angle(\text{aff}(\tau_k^{d-n}), N_q\mathcal{M}) \sin \angle(N_p\mathcal{M}, N_q\mathcal{M})}{\cos \angle(N_p\mathcal{M}, N_q\mathcal{M}) \sin \angle(\text{aff}(\tau_k^{d-n}), T_p\mathcal{M})} \\
 &= \frac{\tan \angle(\text{aff}(\tau_k^{d-n}), N_q\mathcal{M}) \sin \angle(N_p\mathcal{M}, N_q\mathcal{M})}{\cos \angle(N_p\mathcal{M}, N_q\mathcal{M}) \cos \angle(\text{aff}(\tau_k^{d-n}), N_p\mathcal{M})} \\
 &= \frac{\tan \angle(\text{aff}(\tau_k^{d-n}), N_q\mathcal{M}) \tan \angle(N_p\mathcal{M}, N_q\mathcal{M})}{\cos \angle(\text{aff}(\tau_k^{d-n}), N_p\mathcal{M})}.
 \end{aligned} \tag{42}$$

Lemma 25 gives us that $\sin \angle(\text{aff}(\tau_k^{d-n}), T_p\mathcal{M}), \sin \angle(\text{aff}(\tau_k^{d-n}), T_q\mathcal{M}) \geq \frac{16}{13} \alpha_{d-n}$, so that $\cos \angle(\text{aff}(\tau_k^{d-n}), T_q\mathcal{M}) \geq \frac{16}{13} \alpha_{d-n}$ and

$$\tan \angle(\text{aff}(\tau_k^{d-n}), N_q\mathcal{M}) \leq \frac{1 - (\frac{16}{13} \alpha_{d-n})^2}{\frac{16}{13} \alpha_{d-n}}.$$

By Lemma 2

$$\sin \left(\frac{\angle(T_p\mathcal{M}, T_q\mathcal{M})}{2} \right) \leq \frac{|p-q|}{2\text{rch}(\mathcal{M})},$$

so that, using $\tan(2\arcsin(x)) = \frac{2x\sqrt{1-x^2}}{1-2x^2}$,

$$\tan \angle(N_p\mathcal{M}, N_q\mathcal{M}) \leq \frac{\frac{|p-q|}{\text{rch}(\mathcal{M})} \sqrt{1 - \frac{|p-q|^2}{4\text{rch}(\mathcal{M})^2}}}{1 - \frac{|p-q|^2}{2\text{rch}(\mathcal{M})^2}}.$$

This means that (42) yields,

$$|\pi_{v(\tau_k^{d-n}),p}^{-1}(u) - \pi_{v(\tau_k^{d-n}),q}^{-1}(\pi_{N_{q,\mathcal{M}} \rightarrow N_{p,\mathcal{M}}}(u))| \leq \frac{1 - \left(\frac{16}{13}\alpha_{d-n}\right)^2}{\left(\frac{16}{13}\alpha_{d-n}\right)^2} \frac{\frac{|p-q|}{\text{rch}(\mathcal{M})} \sqrt{1 - \frac{|p-q|^2}{4\text{rch}(\mathcal{M})^2}}}{1 - \frac{|p-q|^2}{2\text{rch}(\mathcal{M})^2}}$$

By the triangle inequality (on the terms in the sum in the definition (32)), this gives

$$|N_{\bar{p},p}(u) - N_{\bar{p},q}(\pi_{N_{q,\mathcal{M}} \rightarrow N_{p,\mathcal{M}}}(u))| \leq \frac{1 - \left(\frac{16}{13}\alpha_{d-n}\right)^2}{\left(\frac{16}{13}\alpha_{d-n}\right)^2} \frac{\frac{|p-q|}{\text{rch}(\mathcal{M})} \sqrt{1 - \frac{|p-q|^2}{4\text{rch}(\mathcal{M})^2}}}{1 - \frac{|p-q|^2}{2\text{rch}(\mathcal{M})^2}}$$

Because the u component of $N_{\bar{p},p}(u)$ is u and its length is at least 1, we find that also

$$\sin \angle(N_{\bar{q},p}(u), N_{\bar{q},q}(\pi_{N_{q,\mathcal{M}} \rightarrow N_{p,\mathcal{M}}}(u))) \leq \frac{1 - \left(\frac{16}{13}\alpha_{d-n}\right)^2}{\left(\frac{16}{13}\alpha_{d-n}\right)^2} \frac{\frac{|p-q|}{\text{rch}(\mathcal{M})} \sqrt{1 - \frac{|p-q|^2}{4\text{rch}(\mathcal{M})^2}}}{1 - \frac{|p-q|^2}{2\text{rch}(\mathcal{M})^2}}$$

Because p and q are very close (in fact they lie in an L neighbourhood of τ , which is small due to (15))

$$\frac{\sqrt{1 - \frac{|p-q|^2}{4\text{rch}(\mathcal{M})^2}}}{1 - \frac{|p-q|^2}{2\text{rch}(\mathcal{M})^2}} \leq 2,$$

as can be verified using that $\frac{\sqrt{1-x^2}}{1-2x^2}$ is monotone increasing for sufficiently small x . This means we can simplify the result further

$$\sin \angle(N_{\bar{q},p}(u), N_{\bar{q},q}(\pi_{N_{q,\mathcal{M}} \rightarrow N_{p,\mathcal{M}}}(u))) \leq \left(\frac{10}{16\alpha_{d-n}}\right)^2 \frac{|p-q|}{\text{rch}(\mathcal{M})}$$

Thanks to (41), we now have

$$\angle\left(\text{span}_{u \in N_{p,\mathcal{M}}}(N_{\bar{q},p}(u)), \text{span}_{u \in N_{q,\mathcal{M}}}(N_{\bar{q},q}(u))\right) \leq \arcsin\left(\left(\frac{13}{16\alpha_{d-n}}\right)^2 \frac{|p-q|}{\text{rch}(\mathcal{M})}\right). \quad (43)$$

Step 3: Combining into a bound on $\angle(\mathcal{N}_{\bar{p}}, \mathcal{N}_{\bar{q}})$.

Combining (43), (40), and the triangle inequality, we see that

$$\begin{aligned} & \angle\left(\text{span}_{u \in N_{p,\mathcal{M}}}(N_{\bar{p},p}(u)), \text{span}_{u \in N_{q,\mathcal{M}}}(N_{\bar{q},q}(u))\right) \\ & \leq \angle\left(\text{span}_{u \in N_{p,\mathcal{M}}}(N_{\bar{p},p}(u)), \text{span}_{u \in N_{p,\mathcal{M}}}(N_{\bar{q},p}(u))\right) + \angle\left(\text{span}_{u \in N_{p,\mathcal{M}}}(N_{\bar{q},p}(u)), \text{span}_{u \in N_{q,\mathcal{M}}}(N_{\bar{q},q}(u))\right) \\ & \leq \arcsin\left(\left(\frac{13}{16\alpha_{d-n}}\right)^2 \sqrt{n+1}|\lambda - \lambda'|\right) + \arcsin\left(\left(\frac{13}{16\alpha_{d-n}}\right)^2 \frac{|p-q|}{\text{rch}(\mathcal{M})}\right). \end{aligned}$$

Because we need estimates on $\angle(\mathcal{N}_{\bar{p}}, \mathcal{N}_{\bar{q}})$ we have to set $p = \pi_{\mathcal{M}}(\bar{p})$ and $q = \pi_{\mathcal{M}}(\bar{q})$. To estimate the distance between the two points, we first note that $|\bar{p} - \bar{q}| \leq |\lambda - \lambda'| \tilde{L}$, because \bar{p} and \bar{q} have barycentric coordinates λ and λ' . Thanks to [36, Theorem 4.8 (8)], we have that if $d(x, \mathcal{M}), d(y, \mathcal{M}) \leq \frac{1}{2} \text{rch}(\mathcal{M})$, then $|\pi_{\mathcal{M}}(x) - \pi_{\mathcal{M}}(y)| \leq 2|x - y|$. This means that

$$\begin{aligned} \angle(\mathcal{N}_{\bar{p}}, \mathcal{N}_{\bar{q}}) &= \angle\left(\text{span}_{u \in N_{\pi_{\mathcal{M}}(\bar{p})} \mathcal{M}}(N_{\bar{p}, \pi_{\mathcal{M}}(\bar{p})}(u)), \text{span}_{u \in N_{\pi_{\mathcal{M}}(\bar{q})} \mathcal{M}}(N_{\bar{q}, \pi_{\mathcal{M}}(\bar{q})}(u))\right) \\ &\leq \arcsin\left(\left(\frac{13}{16\alpha_{d-n}}\right)^2 \sqrt{n+1} |\lambda - \lambda'|\right) + \arcsin\left(\left(\frac{13}{16\alpha_{d-n}}\right)^2 \frac{2|\lambda - \lambda'| \tilde{L}}{\text{rch}(\mathcal{M})}\right). \end{aligned}$$

Since $\sin(\arcsin(x) + \arcsin(y)) = \sqrt{1-x^2}y + \sqrt{1-y^2}x \leq x + y$, we see that

$$\sin(\angle(\mathcal{N}_{\bar{p}}, \mathcal{N}_{\bar{q}})) \leq \left(\frac{13}{16\alpha_{d-n}}\right)^2 \sqrt{n+1} |\lambda - \lambda'| + \left(\frac{13}{16\alpha_{d-n}}\right)^2 \frac{2|\lambda - \lambda'| \tilde{L}}{\text{rch}(\mathcal{M})}.$$

Because of (15) and (9),

$$\begin{aligned} \left(\left(\frac{13}{16\alpha_{d-n}}\right)^2 \frac{2|\lambda - \lambda'| \tilde{L}}{\text{rch}(\mathcal{M})}\right) &\leq \left(\frac{13}{16\alpha_{d-n}}\right)^2 4|\lambda - \lambda'| \frac{(\alpha_{d-n})^{4+2n}}{54(n+1)^2} \\ &\leq \frac{6}{100} |\lambda - \lambda'| (\alpha_{d-n})^2. \end{aligned}$$

Thanks to (11), the first term in the following sum is by far the largest

$$\sin(\angle(\mathcal{N}_{\bar{p}}, \mathcal{N}_{\bar{q}})) \leq \left(\frac{13}{16\alpha_{d-n}}\right)^2 \sqrt{n+1} |\lambda - \lambda'| + \frac{6}{100} |\lambda - \lambda'| (\alpha_{d-n})^2,$$

We finally arrive at the following simple, but weaker bound

$$\sin(\angle(\mathcal{N}_{\bar{p}}, \mathcal{N}_{\bar{q}})) \leq \left(\frac{13}{15\alpha_{d-n}}\right)^2 \sqrt{n+1} |\lambda - \lambda'|, \quad (44)$$

Step 4: From angles to a lower bound on the neighbourhood size. We now consider the triangle $\bar{p}\bar{q}x$ and we estimate $|\bar{p}x|$, and $|\bar{q}x|$. We remind ourselves that in the statement of the lemma we defined x as the point where the normal spaces $\mathcal{N}_{\bar{p}}$ and $\mathcal{N}_{\bar{q}}$ first intersect. The following estimate will use:

1. the sine rule
2. the fact that the distance between \bar{p} and \bar{q} , is at least $|\lambda - \lambda'| \min \text{alt}(\sigma) / \sqrt{n}$, thanks to Lemma 5.12 of [13]
3. Lemma 28 to bound $\min \text{alt}(\sigma)$
4. Equation (44), which gives a bound on the angle $\angle \bar{p}x\bar{q}$, namely ϕ_0
5. Lemma 29 gives that

$$\angle(\text{aff}(\sigma^n)^\perp, N_{p, \mathcal{M}}) \leq \arcsin\left(\frac{(\alpha_{d-n})^{4+n}}{6(n+1)} \zeta^n\right) \leq \arcsin\left(\frac{(\alpha_{d-n})^4}{6}\right), \quad (45)$$

where $\text{aff}(\sigma^n)^\perp$ denotes the space perpendicular to $\text{aff}(\sigma^n)$. Because $e_j \in N_{p^*}\mathcal{M}$, combining this with Lemma 25 and the triangle inequality for angles yields

$$\begin{aligned} \angle(N_{\bar{p}'}(e_j), \text{aff}(\sigma^n)^\perp) &\leq \angle(N_{\bar{p}'}(e_j), e_j) + \angle(N_{p^*}\mathcal{M}, \text{aff}(\sigma^n)^\perp) \\ &\leq \arccos\left(\frac{16}{13}\alpha_{d-n}\right) + \arcsin\left(\frac{(\alpha_{d-n})^4}{6}\right). \end{aligned} \quad (46)$$

We need a lower bound on $\sin(\angle\bar{p}qx)$ and $\sin(\angle\bar{q}px)$, that is

$$\sin\angle(N_{\bar{p}'}(e_j), \text{aff}(\sigma^n)) = \cos\angle(N_{\bar{p}'}(e_j), \text{aff}(\sigma^n)^\perp).$$

We also remind ourselves of the trigonometric identity

$$\cos(\arccos(a) + \arcsin(b)) = a\sqrt{1-b^2} - b\sqrt{1-a^2}.$$

Using (46) now gives

$$\begin{aligned} \sin\angle(N_{\bar{p}'}(e_j), \text{aff}(\sigma^n)) &\geq \cos\left(\arccos\left(\frac{16}{13}\alpha_{d-n}\right) + \arcsin\left(\frac{(\alpha_{d-n})^4}{6}\right)\right) \\ &= \left(\frac{16}{13}\alpha_{d-n}\right)\sqrt{1 - \frac{(\alpha_{d-n})^8}{6^2}} - \frac{(\alpha_{d-n})^4}{6}\sqrt{1 - \left(\frac{16}{13}\alpha_{d-n}\right)^2} \\ &\geq \frac{16}{13}\alpha_{d-n} - \left(\frac{16}{13}\alpha_{d-n}\right)\frac{(\alpha_{d-n})^8}{6^2} - \frac{(\alpha_{d-n})^4}{6} \\ &\geq \frac{16}{13}\alpha_{d-n} - \frac{(\alpha_{d-n})}{18^3} \quad (\text{because } \alpha_k \leq \frac{1}{18^k} \text{ by (11)}) \\ &\geq \alpha_{d-n}. \end{aligned} \quad (47)$$

This completes the fifth point.

The considerations we summed up yield:

$$\begin{aligned} |\bar{p}x|, |\bar{q}x| &\geq \frac{(|\lambda - \lambda'| \min \text{alt}(\sigma) / \sqrt{n}) \alpha_{d-n}}{\left(\frac{10}{15\alpha_{d-n}}\right)^2 \sqrt{n+1} |\lambda - \lambda'|} \\ &\geq \frac{\min \text{alt}(\sigma) \alpha_{d-n} \left(\frac{15}{10}\alpha_{d-n}\right)^2}{n+1} \\ &\geq \frac{\alpha_{d-n} \left(\frac{15}{13}\alpha_{d-n}\right)^2}{n+1} (\zeta \alpha_{d-n-1})^n \tilde{L} \end{aligned}$$

Using (47) again yields that the distance from x to $\text{aff}(\sigma^n)$ is bounded from below by

$$d(x, \text{aff}(\sigma^n)) \geq \frac{(\alpha_{d-n})^2 \left(\frac{15}{13}\alpha_{d-n}\right)^2}{n+1} (\zeta \alpha_{d-n-1})^n \tilde{L}.$$

This completes the proof. \square

Lemma 31 *Suppose $\tau^d \in \mathcal{T}$ and that $\mathcal{M} \cap \tau^d \neq \emptyset$. Then, $\mathcal{M} \cap \tau^d$ lies in the tubular neighbourhood of $K \cap \tau^d$ as defined in Section 7.1 (whose size is lower bounded by Lemma 30).*

Proof Consider $v(\tau^d) \subset K \cap \tau^d$, where we use the definition (28) and choose an arbitrary n dimensional simplex $\sigma^n \subset K \cap \tau^d$. Note that $v(\tau^d) \in K \cap \tau^d$. Thanks to Lemma 29,

$$\sin \angle(\text{aff}(\sigma^n), T_v \mathcal{M}) \leq \frac{(\alpha_{d-n})^{4+n}}{6(n+1)} \zeta^n.$$

From this bound we conclude that

$$d_H(T_v \mathcal{M} \cap B(v, 2L), \text{aff}(\sigma^n) \cap B(v, 2L)) \leq 2 \frac{(\alpha_{d-n})^{4+n}}{6(n+1)} \zeta^n L,$$

where d_H denotes the Hausdorff distance. Because of Lemma 6 and (13), we have that

$$d_H(T_v \mathcal{M} \cap B(v, 2L), \pi_v^{-1}(B_{T_v \mathcal{M}}(v, 2L))) \leq \frac{(\alpha_{d-n})^{4+2n}}{6(n+1)^2} \zeta^{2n} L,$$

where $B_{T_v \mathcal{M}}(v, 2L)$ denotes the ball in $T_v \mathcal{M}$ with centre v and radius $2L$. This gives us

$$\begin{aligned} & d_H(\text{aff}(\sigma^n) \cap B(v, 2L), \pi_v^{-1}(B_{T_v \mathcal{M}}(v, 2L))) \\ & \leq 2 \frac{(\alpha_{d-n})^{4+n}}{6(n+1)} \zeta^n L + \frac{(\alpha_{d-n})^{4+2n}}{6(n+1)^2} \zeta^{2n} L \quad (\text{by the triangle inequality}) \\ & \leq \frac{(\alpha_{d-n})^{4+n} \zeta^n}{n+1} L. \end{aligned}$$

Because $\mathcal{M} \cap \tau \subset \pi_v^{-1}(B_{T_v \mathcal{M}}(v, 2L))$ and the distance between $M \cap \tau$ and $\text{aff}(\sigma^n)$ is small compared to the size of the neighbourhood of K given in Lemma 30, that is

$$\frac{(\alpha_{d-n})^{4+n} \zeta^n}{n+1} L \leq \frac{(\frac{15}{13})^2 (\alpha_{d-n})^4}{n+1} \zeta^n (\alpha_{d-n-1})^n \tilde{L}, \quad (48)$$

$\mathcal{M} \cap \tau$ is contained in this neighbourhood of K . \square

Having established that \mathcal{M} lies in the tubular neighbourhood around K we can sensibly speak about the projection from \mathcal{M} to K along the direction N . Because we also have that the projection from \mathcal{M} to K in the direction \mathcal{N} (as defined in Section 7.1) is transversal (Because $\pi/2$ minus the angle between $\mathcal{N}_{\tilde{p}}$ and $N_p \mathcal{M}$, see (37), is much bigger than the variation of the tangent/normal space as bounded by Lemma 2 and (14)) we see that $\mathcal{M} \cap \tau^d$ is homeomorphic to $K \cap \tau^d$. By construction the projection map is compatible on the boundaries of τ^d , so we also immediately have an explicit homeomorphism between \mathcal{M} and K . Moreover this homeomorphism is piecewise smooth and not just continuous. This completes the proof of Theorem 1. We emphasize that along the way we have also given bounds on

- the Hausdorff distance between \mathcal{M} and K , Lemmas 31 and 30
- the quality of simplices, see Lemma 28
- the variation of the tangent spaces, see Lemma 2 and equations (37), and (14).

Acknowledgments

We thank the reviewers for their comments, which helped to improve the exposition.

References

1. Eddie Aamari, Jisu Kim, Frédéric Chazal, Bertrand Michel, Alessandro Rinaldo, and Larry Wasserman. Estimating the reach of a manifold. *Electron. J. Statist.*, 13(1):1359–1399, 2019.
2. Eddie Aamari and Clément Levrard. Nonasymptotic rates for manifold, tangent space and curvature estimation. *Ann. Statist.*, 47(1):177–204, 02 2019.
3. Milton Abramowitz and Irene A. Stegun. *Handbook of mathematical functions : with formulas, graphs, and mathematical tables*. National Bureau of Standards, 1970.
4. Eugene L. Allgower and Kurt Georg. *Numerical continuation methods: an introduction*, volume 13. Springer Science & Business Media, 1990.
5. Eugene L. Allgower and Phillip H Schmidt. An algorithm for piecewise-linear approximation of an implicitly defined manifold. *SIAM journal on numerical analysis*, 22(2):322–346, 1985.
6. Marek Behr. Simplex spacetime meshes in finite element simulations. *International Journal for Numerical Methods in Fluids*, 57(9):1421–1434, 2008.
7. P. Bendich, S. Mukherjee, and B. Wang. Stratification learning through homology inference. In *2010 AAAI Fall Symposium Series*, 2010.
8. Paul Bendich, David Cohen-Steiner, Herbert Edelsbrunner, John Harer, and Dmitriy Morozov. Inferring local homology from sampled stratified spaces. In *Proc. of the IEEE Symp. on Foundations of Computer Science*, pages 536–546, 2007.
9. Matthew Berger, Andrea Tagliasacchi, Lee M. Seversky, Pierre Alliez, Joshua A. Levine, Andrei Sharf, and Claudio T. Silva. State of the Art in Surface Reconstruction from Point Clouds. In Sylvain Lefebvre and Michela Spagnuolo, editors, *Eurographics 2014 - State of the Art Reports*. The Eurographics Association, 2014.
10. J.-D. Boissonnat, D. Cohen-Steiner, B. Mourrain, G. Rote, and G. Vegter. Meshing of surfaces. In J.-D. Boissonnat and M. Teillaud, editors, *Effective Computational Geometry for Curves and Surfaces*. Springer, 2006.
11. J.-D. Boissonnat, R. Dyer, and A. Ghosh. The stability of Delaunay triangulations. *International Journal of Computational Geometry & Applications*, 23(04n05):303–333, 2013.
12. J.-D. Boissonnat, R. Dyer, and A. Ghosh. Delaunay stability via perturbations. *International Journal of Computational Geometry & Applications*, 24(02):125–152, 2014.
13. Jean-Daniel Boissonnat, Frédéric Chazal, and Mariette Yvinec. *Geometric and Topological Inference*. Cambridge Texts in Applied Mathematics. Cambridge University Press, 2018.

14. Jean-Daniel Boissonnat, David Cohen-Steiner, and Gert Vegter. Isotopic implicit surface meshing. *Discrete & Computational Geometry*, 39(1):138–157, Mar 2008.
15. Jean-Daniel Boissonnat, Ramsay Dyer, Arijit Ghosh, and Mathijs Wintraecken. Local Criteria for Triangulation of Manifolds. In Bettina Speckmann and Csaba D. Tóth, editors, *34th International Symposium on Computational Geometry (SoCG 2018)*, volume 99 of *Leibniz International Proceedings in Informatics (LIPIcs)*, pages 9:1–9:14, Dagstuhl, Germany, 2018. Schloss Dagstuhl–Leibniz-Zentrum fuer Informatik.
16. Jean-Daniel Boissonnat and Arijit Ghosh. Manifold reconstruction using tangential Delaunay complexes. *Discrete & Computational Geometry*, pages 221–267, 2014.
17. Jean-Daniel Boissonnat, Siargey Kachanovich, and Mathijs Wintraecken. Sampling and Meshing Submanifolds in High Dimension. hal-02386169, November 2019.
18. Jean-Daniel Boissonnat, André Lieutier, and Mathijs Wintraecken. The Reach, Metric Distortion, Geodesic Convexity and the Variation of Tangent Spaces. *Journal of Applied and Computational Topology volume*, 3:29–58, 2019.
19. Adam Brown and Bei Wang. Sheaf-Theoretic Stratification Learning. In Bettina Speckmann and Csaba D. Tóth, editors, *34th International Symposium on Computational Geometry (SoCG 2018)*, volume 99 of *Leibniz International Proceedings in Informatics (LIPIcs)*, pages 14:1–14:14, Dagstuhl, Germany, 2018. Schloss Dagstuhl–Leibniz-Zentrum fuer Informatik.
20. S. S. Cairns. On the triangulation of regular loci. *Annals of Mathematics. Second Series*, 35(3):579–587, 1934.
21. F. Cazals and J. Giesen. Delaunay triangulation based surface reconstruction. In J.-D. Boissonnat and M. Teillaud, editors, *Effective Computational Geometry for Curves and Surfaces*. Springer, 2006.
22. H.-L. Cheng, T. K. Dey, H. Edelsbrunner, and J. Sullivan. Dynamic skin triangulation. *Discrete & Computational Geometry*, 25(4):525–568, Apr 2001.
23. S.-W. Cheng, T. K. Dey, and E. A. Ramos. Manifold Reconstruction from Point Samples. In *Proc. ACM-SIAM Symp. Discrete Algorithms*, pages 1018–1027, 2005.
24. S.-W. Cheng, T. K. Dey, and J. R. Shewchuk. *Delaunay Mesh Generation*. Computer and information science series. CRC Press, 2013.
25. Aruni Choudhary, Siargey Kachanovich, and Mathijs Wintraecken. Coxeter triangulations have good quality. HAL preprint, December 2017.
26. H.S.M. Coxeter. Discrete groups generated by reflections. *Annals of Mathematics*, pages 588–621, 1934.
27. T. K. Dey. *Curve and Surface Reconstruction; Algorithms with Mathematical Analysis*. Cambridge University Press, 2007.
28. Tamal K. Dey and Joshua A. Levine. Delaunay meshing of piecewise smooth complexes without expensive predicates. *Algorithms*, 2(4):1327–1349, 2009.
29. Tamal K. Dey and Andrew G. Slatton. Localized delaunay refinement for volumes. *Computer Graphics Forum*, 30(5):1417–1426, 2011.

30. Tamal K. Dey and Jian Sun. Normal and feature approximations from noisy point clouds. In S. Arun-Kumar and Naveen Garg, editors, *FSTTCS 2006: Foundations of Software Technology and Theoretical Computer Science*, pages 21–32, Berlin, Heidelberg, 2006. Springer Berlin Heidelberg.
31. T.K. Dey and A. Slatton. Localized delaunay refinement for piecewise-smooth complexes. *SoCG*, 2013.
32. Akio Doi and Akio Koide. An efficient method of triangulating equi-valued surfaces by using tetrahedral cells. *IEICE TRANSACTIONS on Information and Systems*, E74-D, 1991.
33. J.J. Duistermaat and J.A.C. Kolk. *Multivariable Real Analysis II: Integration*. Cambridge University Press, 2004.
34. R. Dyer, G. Vegter, and M. Wintraecken. Riemannian simplices and triangulations. *Geometriae Dedicata*, 179(1):91–138, 2015. (Preprint: arXiv:1406.3740).
35. H. Edelsbrunner and N. R. Shah. Triangulating topological spaces. In *SoCG*, pages 285–292, 1994.
36. H. Federer. Curvature measures. *Trans. Amer. Math. Soc.*, 93(3):418–491, 1959.
37. M. W. Hirsch. *Differential Topology*. Springer-Verlag, 1976.
38. Siargey Kachanovich. *Meshing submanifolds using Coxeter triangulations*. Theses, Université Côte d’Azur, October 2019.
39. William E Lorensen and Harvey E Cline. Marching cubes: A high resolution 3d surface construction algorithm. In *ACM siggraph computer graphics*, volume 21, pages 163–169. ACM, 1987.
40. Albert T. Lundell and Stephen Weingram. *The Topology of CW Complexes*. Van Nostrand Reinhold Company, 1969.
41. Maurice Maes and Bert Kappen. On the permutahedron and the quadratic placement problem. *Philips Journal of Research*, 46(6):267–292, 1992.
42. P. Niyogi, S. Smale, and S. Weinberger. Finding the homology of submanifolds with high confidence from random samples. *Discrete & Comp. Geom.*, 39(1-3):419–441, 2008.
43. Steve Oudot, Laurent Rineau, and Mariette Yvinec. Meshing Volumes Bounded by Smooth Surfaces. *Computational Geometry, Theory and Applications*, 38:100–110, 2007.
44. Simon Plantinga and Gert Vegter. Isotopic approximation of implicit curves and surfaces. In *Proceedings of the 2004 Eurographics/ACM SIGGRAPH symposium on Geometry processing*, pages 245–254. ACM, 2004.
45. B.C. Rennie and A.J. Dobson. On Stirling numbers of the second kind. *Journal of Combinatorial Theory*, 7(2):116 – 121, 1969.
46. Laurent Rineau. *Meshing Volumes bounded by Piecewise Smooth Surfaces*. Theses, Université Paris-Diderot - Paris VII, November 2007.
47. C.P. Rourke and B.J. Sanderson. *Introduction to piecewise-linear topology*. Number 69 in *Ergebnisse der mathematik und ihrer grenzgebiete*. Springer-Verlag, 1972.
48. J. R. Shewchuk. What is a good linear finite element? - interpolation, conditioning, anisotropy, and quality measures. <http://www.cs.berkeley.edu/~jrs/papers/lelmj.pdf> (last viewed 2008), 2002.

49. Max von Danwitz, Violeta Karyofylli, Norbert Hosters, and Marek Behr. Simplex space-time meshes in compressible flow simulations. *International Journal for Numerical Methods in Fluids*, 91(1):29–48, 2019.
50. J. G. Wendel. Note on the gamma function. *The American Mathematical Monthly*, 55(9):563–564, 1948.
51. J. H. C. Whitehead. On C^1 -complexes. *Annals of Mathematics*, 41(4):809–824, 1940.
52. H. Whitney. *Geometric Integration Theory*. Princeton University Press, 1957.

A Notation

In the following table we give an overview of the notation used in this paper and compare it to Whitney's notation.

Notation	definition	Whitney's notation (if relevant)
A_i	Affine subspaces	P, P' and Q
aff	The affine hull	
$B^d(c, r)$	A ball with in \mathbb{R}^d of dimension with centre c and radius r , if we do not need to emphasize the centre or radius or they are to be determined, these are suppressed from the notation	$U_r(c)$
$B_{T_p \mathcal{M}}(c, r)$	A ball in $T_p \mathcal{M}$, using the same conventions as for $B^d(c, r)$	
$\mathring{C}(T_p \mathcal{M}, r_1, r_2)$	Open cylinder given by all points that project orthogonally onto an open ball of radius r_1 in $T_p \mathcal{M}$ and whose distance to this ball is at most r_2	
$\tilde{c}L$	Perturbation radius of the vertices of \mathcal{T}	ρ
\tilde{c}	Normalized perturbation radius	ρ^*
d	Ambient dimension (\mathbb{R}^d)	m
$d(\cdot, \cdot)$	Euclidean distance between sets	
$d_{\mathcal{M}}(\cdot, \cdot)$	Distance on \mathcal{M}	
δ	Protection	
ε	The sampling density as in an (ε, μ) -net (the circumradius of the simplices in the Coxeter triangulation)	
K	Triangulation of \mathcal{M}	K
$L(\cdot)$	Longest edge length	δ is the longest edge length of the ambient triangulation L
L	$L = L(\mathcal{T})$	
\tilde{L}	$\tilde{L} = L(\tilde{\mathcal{T}})$	
λ	barycentric coordinates	
\mathcal{M}	The manifold	M
μ	Separation as in an (ε, μ) -net (the shortest edge length in \mathcal{T} for Coxeter triangulations)	
μ_0	The normalized separation, that is $\mu = \mu_0 \varepsilon$	
n	Dimension of \mathcal{M}	n
$N_{\mathcal{M}}, N_p \mathcal{M}$	The normal bundle and normal space at p	
$N_{\leq k}$	An upper bound on the total number of faces of dimension less or equal to k that contain a given vertex.	Whitney does not distinguish dimensions and uses N as an upper bound. (no value given)
$N_{v(\tau)}(e_i)$	See (32)	
$\mathcal{N}_{\bar{p}}$	The 'normal' space of K at \bar{p} , that is $\text{span}(N_{\bar{p}}(e_i))$	
$\pi_{\mathcal{M}}$	Closest point projection on \mathcal{M}	π^*
$\pi_{T_p \mathcal{M}}$	Orthogonal projection on the tangent spaces $T_p \mathcal{M}$	
π_p^{-1}	See Definition 4	
$\pi_{\text{aff}(\tau_k^{d-n}) \rightarrow N_p \mathcal{M}} =$	The orthogonal projection map from the affine hull $\text{aff}(\tau_k^{d-n})$ to $N_p \mathcal{M}$.	
$\pi_{\tau_k^{d-n}}$		
$\text{rch}(\mathcal{M})$	The reach to the manifold \mathcal{M}	
$\bar{\rho}_1$	Volume fraction of the part of a ball inside a slab	ρ_1
ρ_1	Lower bound on $\bar{\rho}_1$, see (7)	
\mathcal{S}	Slab between two hyperplanes intersected with a ball	Q'

$T\mathcal{M}, T_p\mathcal{M}$ \mathcal{T}	The tangent bundle and the tangent space at p The ambient Coxeter triangulation of type \tilde{A}	P_p L is the ambient triangulation, but is not a Coxeter triangulation
$\tilde{\mathcal{T}}$ τ, σ	Perturbed ambient triangulation Simplices. We have tried to reserve τ for \mathcal{T} or $\tilde{\mathcal{T}}$ and σ for K . However for arbitrary simplices (such as in Appendix B) we use arbitrary choices. Subscripts are used for indices and superscripts for the dimension.	L^* Same
$t(\sigma)$ $U(X, r)$	Thickness of σ A neighbourhood of radius r of a set X	$U_r(X)$
v_i v_i^*	Vertices of \mathcal{T} Vertices of $\tilde{\mathcal{T}}$	p_i p_i^*

Overview most important bounds

We recall here for the reader's convenience the most important bounds and constants used in the paper.

The constant $\bar{\rho}_1 > 0$ (depending only on d) is defined as follows: For any two parallel $(d-1)$ -hyperplanes whose distance apart is less than $2\bar{\rho}_1 r$, the intersection of the slab between the two hyperplanes with the ball $B^d(r)$ is denoted by \mathcal{S} . Now, $\bar{\rho}_1$ is the largest number such that the volume (vol) of any \mathcal{S} satisfies

$$\text{vol}(\mathcal{S}) \leq \frac{\text{vol}(B^d(r))}{2N_{\leq d-n-1}},$$

where $N_{\leq k}$ is an upper bound on the total number of faces of dimension less or equal to k that contain a given vertex, see (6).

α_1 and α_k have been defined by a recursion relation as follows

$$\alpha_1 = \frac{4}{3}\rho_1\tilde{c} \quad \frac{2}{3}\alpha_{k-1}\tilde{c}\rho_1 = \alpha_k, \quad (10)$$

and thus $\alpha_k = \frac{2^{k+1}}{3^k}\rho_1^k\tilde{c}^k$. In particular, we have the bound

$$\alpha_k \leq \frac{1}{18^k}. \quad (11)$$

L satisfies

$$\left(1 - \sqrt{1 - \left(\frac{6L(\mathcal{T})}{\text{rch}(\mathcal{M})}\right)^2}\right) \text{rch}(\mathcal{M}) = \frac{(\alpha_{d-n})^{4+2n}}{6(n+1)^2} \zeta^{2n} L \quad (13)$$

or equivalently

$$\frac{L}{\text{rch}(\mathcal{M})} = \frac{2 \frac{(\alpha_{d-n})^{4+2n}}{6(n+1)^2} \zeta^{2n}}{\left(\frac{(\alpha_{d-n})^{4+2n}}{6(n+1)^2} \zeta^{2n}\right)^2 + 6^2}, \quad (14)$$

with

$$\zeta = \frac{8}{15\sqrt{d} \binom{d}{d-n} \cdot (1+2\tilde{c})} \left(1 - \frac{8\tilde{c}}{t(\mathcal{T})^2}\right) t(\mathcal{T}). \quad (12)$$

We often use

$$\frac{L}{\text{rch}(\mathcal{M})} < \frac{(\alpha_{d-n})^{4+2n}}{54(n+1)^2} \zeta^n < \frac{(\alpha_{d-n})^2}{54}, \quad \frac{(\alpha_{d-n})^{4+2n}}{6(n+1)^2} \zeta^{2n} < \frac{(\alpha_{d-n})^2}{3} \leq \frac{\alpha_{d-n}}{3}. \quad (15)$$

The normalized perturbation radius \tilde{c} satisfies

$$|v_i - \tilde{v}_i| \leq \tilde{c}L = \min \left\{ \frac{t(\mathcal{T})\mu_0}{18d} \delta, \frac{1}{24} t(\mathcal{T})^2 L \right\}, \quad (19)$$

from which it follows that

$$\tilde{c} \leq \frac{1}{24}. \quad (9)$$

B Some properties of affine spaces

In this appendix, we discuss two variants of lemmas from Appendix Section II.14 of [52], that are essential in the building of the triangulation, see Section 6.1 in particular. Both lemmas are due to Whitney. However, in both cases, the statement is different, because we prefer to work directly with angles and use the thickness as our quality measure. In the first case, the proof we provide differs significantly from the original. The first lemma will allow us to prove that if $T_p \mathcal{M}$ intersects a simplex $\tau \in \mathcal{T}$ and p and τ are not too far from each other then \mathcal{M} intersects τ and vice versa. The second result is essential in proving that the perturbation of the vertices as described in Section 2.1 part 1, gives a triangulation for which the low dimensional simplices are sufficiently far away from the manifold.

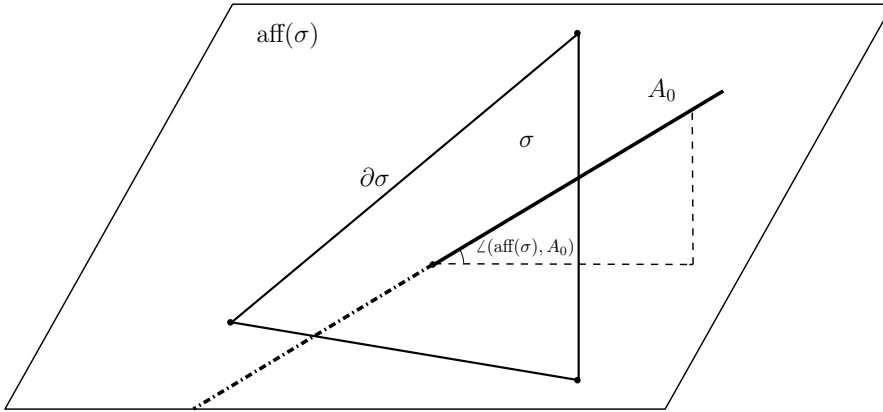


Fig. 9 An illustration of the notation of Lemma 32.

We start with a variation on Lemma 14a of Appendix Section II.14 of [52].

Lemma 32 *Let σ be an s -simplex and A_0 an affine n -dimensional subspace in \mathbb{R}^d . Assume that $s+n \geq d$ and*

$$d(A_0, \sigma) < d(A_0, \partial\sigma).$$

Then $s+n = d$, A_0 intersects σ in a single point and

$$\sin \angle(\text{aff}(\sigma), A_0) \geq 2d(A_0, \partial\sigma)/L(\sigma).$$

Proof of Lemma 32 Choose $p \in \sigma$ and $q \in A_0$ such that

$$|p - q| = d(A_0, \sigma).$$

Now suppose that there is a vector $v \neq 0$ that lies in the intersection of $\text{aff}(\sigma)$ and A_0 . Then there exists some $c \in \mathbb{R}$ such that $p + cv \in \partial\sigma$. Because v lies in the intersection of $\text{aff}(\sigma)$ and A_0 , we have that $q + cv \in A_0$. Clearly translation leaves distances invariant, so

$$d(A_0, \sigma) = |p - q| = |(p + cv) - (q + cv)| \geq d(A_0, \partial\sigma),$$

which clearly contradicts the assumption. This means we can conclude that there is no such v and therefore $s + n = d$.

Because there is no v in the intersection of $\text{aff}(\sigma)$ and A_0 , there is a unique point \bar{p} in this intersection. We'll now show that $\bar{p} \in \sigma$. I'll assume that $\bar{p} \notin \sigma$. This means in particular that $q \neq \bar{p}$. Because $d(A_0, \sigma) < d(A_0, \partial\sigma)$, $p - q$ is normal to $\text{aff}(\sigma)$ and $p \in \sigma \setminus \partial\sigma$. Now consider the line from q to \bar{p} , which lies in A_0 . The distance from a point on this line to σ decreases (at least at first) as you go from q toward \bar{p} . This contradicts the definition of q . We conclude that $\bar{p} \in \sigma$.

Now suppose that l_0 is a line in A_0 that goes through \bar{p} . In order to derive a contradiction, we assume that

$$\sin \phi < 2d(A_0, \partial\sigma)/L(\sigma),$$

where $\sin \phi$ denotes the angle between l_0 and $\text{aff}(\sigma)$. Denote by $\pi_{\text{aff}(\sigma)}(l_0)$ the orthogonal/closest point projection on $\text{aff}(\sigma)$ of l_0 . Because $\bar{p} \in \sigma$ $\pi_{\text{aff}(\sigma)}(l_0)$ intersects $\partial\sigma$ at a point \bar{q} and we may assume that $|\bar{p} - \bar{q}| \leq \frac{1}{2}L(\sigma)$ so that l_0 contains a point a distance

$$\frac{1}{2}L(\sigma) \sin \phi < \frac{1}{2}L(\sigma)2d(A_0, \partial\sigma)/L(\sigma) = d(A_0, \partial\sigma)$$

from $\partial\sigma$, a contradiction. Because l_0 was an arbitrary line in A_0 the result now follows. \square

The following is a variation on Lemma 14b of Appendix Section II.14 of [52]. The proof presented here is almost identical to the original.

Lemma 33 *Let A_1 and A_2 be two affine subspaces in \mathbb{R}^d , with $A_1 \subset A_2$. Let τ be a simplex in A_2 , and let v be a point in $\mathbb{R}^d \setminus \tau$. Define J to be the join of τ and v . Then*

$$d(J, A_1) \geq \frac{d(\tau, A_1)d(v, A_2)}{L(J)}, \quad (49)$$

where the distances between sets are defined as $d(B, C) = \inf_{x \in B, y \in C} |x - y|$ and $L(J)$ denotes the longest edge length of an edge in J .

Proof of Lemma 33 Let us suppose that (49) is false. Let J^c be the truncated cone that consists of all half-lines that start at a point of τ and pass through v . Then we may choose $p_J \in J^c$ and $a_1 \in A_1$ so that

$$|p_J - a_1| = d(J^c, A_1),$$

by the definition of J^c and the hypothesis we also have

$$d(J^c, A_1) \leq d(J, A_1) < \frac{d(\tau, A_1)d(v, A_2)}{L(J)}. \quad (50)$$

Now suppose that p_J lies on the half line that starts at $w \in \tau$ and goes through v . Because $\tau \subset A_2$, we see that $d(v, A_2) \leq L_e(J)$. This means that (50) gives that $d(J^c, A_1) < d(\tau, A_1)$, so that $p_J \neq w$. We now immediately see that the line segment $a_1 p_J$ is orthogonal to the line that goes through w and v , which extends the half line we mentioned above. Let ℓ now be the line that goes through a_1 and w , and $\pi_\ell(v) \in \ell$ the point that is closest to v . It follows that $\pi_\ell(v)w$ is perpendicular to ℓ . Because a_1 is nearer to p_J than w , a_1 and $\pi_\ell(v)$ are on the same side of w in ℓ . This means because two of the angles are the same (and thus the third), that the triangles $p_J w a_1$ and $\pi_\ell(v) w v$ are similar. We now have that

$$d(J^c, A_1) = |p_J - a_1| = \frac{|a_1 - w||v - \pi_\ell(v)|}{|v - w|} \geq \frac{d(\tau, A_1)d(v, A_2)}{L(J)},$$

contradicting the hypothesis and thus proving the lemma. \square

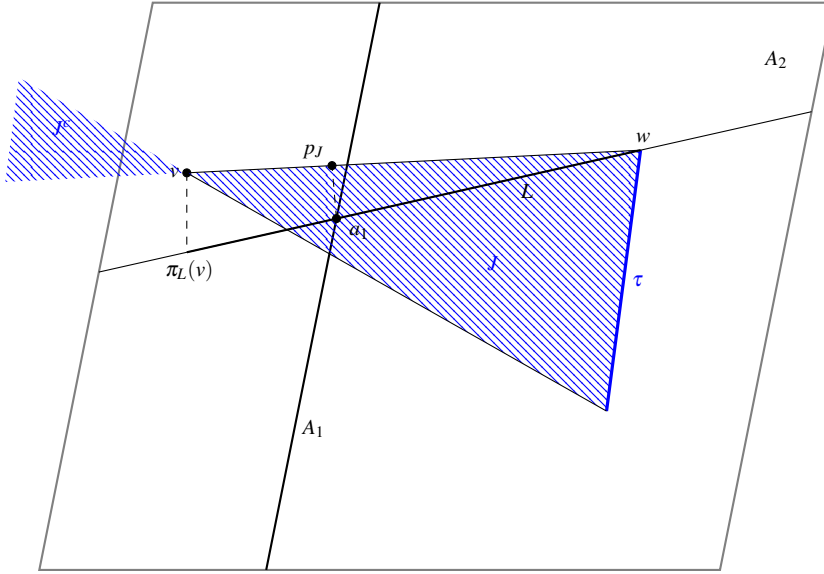


Fig. 10 Notation for the proof of Lemma 33.

C Remark on the $C^{1,1}$ case

We now first discuss a simpler version of Lemma 3 before going in to the $C^{1,1}$ setting. The result in this case is weaker, but can be easily extended to the $C^{1,1}$ setting as we shall see below.

The following consequence of Lemma 2 of is a stronger version of Lemma 5.4 of [42]:

Corollary 34 *Suppose \mathcal{M} is C^2 and $p \in \mathcal{M}$, then for all $0 < r < \frac{\text{rch}(\mathcal{M})}{\sqrt{2}}$, the projection $\pi_{T_p \mathcal{M}}$ onto the tangent space $T_p \mathcal{M}$, restricted to $\mathcal{M} \cap B(p, r)$ is a diffeomorphism onto its image.*

Proof Let $q \in \mathcal{M}$ such that $|p - q| \leq r$, then the differential of the projection map $\pi_{T_p \mathcal{M}}$ at q is non-degenerate, because by Lemma 2, the angle $\angle(T_p \mathcal{M}, T_q \mathcal{M})$ is less than $\pi/2$. Because $\mathcal{M} \cap B(p, r)$ is a topological ball of the right dimension by Proposition 1 of [18], the result now follows. \square

Similarly to Lemma 2 we have for $C^{1,1}$ manifolds that:

Lemma 35 (Theorem 3 of [18]) *Now suppose that \mathcal{M} has positive reach, that is \mathcal{M} is at least $C^{1,1}$, and let $|p - q| \leq \text{rch}(\mathcal{M})/3$, then*

$$\sin \frac{\angle(T_p \mathcal{M}, T_q \mathcal{M})}{2} \leq \frac{1 - \sqrt{1 - \alpha^2}}{\sqrt{\frac{\alpha^2}{4} - (\frac{\alpha^2}{2} + 1 - \sqrt{1 - \alpha^2})^2}},$$

where $\alpha = |p - q|/\text{rch}(\mathcal{M})$.

This lemma gives us a corollary, which is the equivalent of Corollary 34:

Corollary 36 *Suppose \mathcal{M} is $C^{1,1}$ and $p \in \mathcal{M}$, then for all $r < \frac{\text{rch}(\mathcal{M})}{3}$, the projection $\pi_{T_p \mathcal{M}}$ onto the tangent space $T_p \mathcal{M}$, restricted to $\mathcal{M} \cap B(p, r)$ is a diffeomorphism onto its image.*

These are in fact all the fundamental results that are needed to be able to extend to the $C^{1,1}$ setting.

Assuming the manifold is $C^{1,1}$ would lead to minor changes in the calculations in the proof of Lemma 26 and would in theory influence the final conclusion in Section 7.2. However, because we have a significant margin in the difference between $\pi/2$ minus the angle between $\mathcal{N}_{\bar{p}}$ and $N_p \mathcal{M}$ we would not need to change the constants in Section 7.2. Because we use the projection on the manifold, which is only Lipschitz, the map is homeomorphism is no longer piecewise smooth, but just Lipschitz. The rest of proofs hold verbatim.